Atmos. Chem. Phys. Discuss., 14, 26803–26855, 2014
www.atmos-chem-phys-discuss.net/14/26803/2014/
doi:10.5194/acpd-14-26803-2014

Atmospheric Chemistry and Physics Discussions
Open Access

This discussion paper is/has been under review for the journal Atmospheric Chemistry and Physics (ACP). Please refer to the corresponding final paper in ACP if available.

Evaluating the effects of China's pollution control on inter-annual trends and uncertainties of atmospheric mercury emissions

Y. Zhao[1], H. Zhong[1], J. Zhang[2], and C. P. Nielsen[3]

[1]State Key Laboratory of Pollution Control & Resource Reuse and School of the Environment, Nanjing University, 163 Xianlin Ave., Nanjing, Jiangsu 210023, China
[2]Jiangsu Provincial Academy of Environmental Science, 241 West Fenghuang St., Nanjing, Jiangsu 210036, China
[3]Harvard China Project, School of Engineering and Applied Sciences, Harvard University, 29 Oxford St, Cambridge, MA 02138, USA

Received: 20 September 2014 – Accepted: 3 October 2014 – Published: 27 October 2014

Correspondence to: Y. Zhao (yuzhao@nju.edu.cn)

Published by Copernicus Publications on behalf of the European Geosciences Union.

Abstract

China's atmospheric mercury (Hg) emissions of anthropogenic origin have been effectively restrained through the national policy of air pollution control. Improved methods based on available field measurements are developed to quantify the benefits of Hg abatement through various emission control measures. Those measures include increased use of flue gas desulfurization (FGD) and selective catalyst reduction (SCR) systems for power sector, precalciners with fabric filter (FF) for cement production, machinery coking with electrostatic precipitator (ESP) for iron and steel production, and advanced manufacturing technologies for nonferrous metal smelting. Declining trends in emissions factors for those sources are revealed, leading to a much slower growth of national total Hg emissions than that of energy and economy, from 679 in 2005 to 750 metric tons (t) in 2012. In particular, nearly half of emissions from the above-mentioned four types of sources are expected to be reduced in 2012, attributed to expansion of technologies with high energy efficiencies and air pollutant removal rates after 2005. The speciation of Hg emissions keeps stable for recent years, with the mass fractions of around 55, 39 and 6 % for Hg^0, Hg^{2+} and Hg^p, respectively. The lower estimate of Hg emissions than previous inventories is supported by limited chemistry simulation work, but middle-to-long term observation on ambient Hg levels is further needed to justify the inter-annual trends of estimated Hg emissions. With improved implementation of emission controls and energy saving, 23 % reduction in annual Hg emissions for the most optimistic case in 2030 is expected compared to 2012, with total emissions below 600 t. While Hg emissions are evaluated to be gradually constrained, increased uncertainties are quantified with Monte-Carlo simulation for recent years, particularly for power and certain industrial sources. The uncertainty of Hg emissions from coal-fired power plants, as an example, increased from −48∼ +73 % in 2005 to −50∼ +89 % in 2012 (expressed as 95 % confidence interval). This is attributed mainly to swiftly increased penetration of advanced manufacturing and pollutant control technologies. The unclear operation status or relatively small sample size of field measurements on

ACPD
14, 26803–26855, 2014

The effects of China's pollution control on atmospheric Hg emissions

Y. Zhao et al.

those technologies results in lower but highly varied emission factors. To further confirm the benefits of pollution control polices with reduced uncertainty, therefore, systematic investigations are recommended specific for Hg pollution sources, and the variability of temporal trends and spatial distributions of Hg emissions need to be better tracked for the country under dramatic changes in economy, energy and air pollution status.

1 Introduction

Increasing international attentions and efforts have been made on study and control of mercury (Hg), a well-known pollutant due to its toxicity and long-range transport. Atmospheric release is identified as the most significant for Hg emissions (Pirrone and Mason, 2009). Different from other heavy metals that are mainly associated with air particles, atmospheric Hg includes the gaseous elemental Hg (GEM, Hg^0) that has longest lifetime and transport distance, reactive gaseous mercury (RGM, Hg^{2+}) that is more affected by local sources, and particle-bound mercury (PBM, Hg^p).

Coal combustion is major source of anthropogenic Hg. As its energy supply is dominated by coal, China's atmospheric Hg emissions from coal combustion have been analyzed by series of studies since late 1990s (Wang et al., 2000; Streets et al., 2005; Wu et al., 2006; Pacyna et al., 2010; Tian et al., 2010). Pacyna et al. (2010) calculated the national emissions from fossil fuel use at 400 metric tons (t) in 2005, accounting for almost half of the country's anthropogenic emissions. In recent years, research focus has been broadened from coal combustion to other industrial and residential sectors including cement (Li, 2011), metal mining and smelting (P. Li et al., 2009; Li et al. 2012, 2010; Wang et al., 2010a; Wu et al., 2012), solid waste incinerator (L. Chen et al., 2013; Hu et al., 2012) and biomass burning (C. Chen et al., 2013; Huang et al., 2011). Growing domestic field measurements have been conducted for those sources and the results are expected to be applied for improving estimate of China's anthropogenic Hg emissions. Current available emission inventory studies indicate that China has become the country with the highest anthropogenic Hg emissions over the world (Fu

ACPD
14, 26803–26855, 2014

et al., 2012a; Pacyna et al., 2010; Pirrone et al., 2010) as well as some other criteria pollutants like SO_2 and NO_X, attributed largely to big and fast growing industrial economy and intensive use of fossil fuels.

Under big pressure to improve air quality, China's government has been implementing series of comprehensive national policy of energy conservation and emission control. Since 2005, for example, the small and inefficient plants or boilers in the power sector and certain heavy industrial sectors including cement and steel production have been gradually replaced with larger, energy-efficient ones with advanced dust collectors; and flue gas desulfurization (FGD) systems have been compulsorily installed at all newly built thermal power units for SO_2 emission abatement (Zhao et al., 2008, 2013). Given the recent serious urban air pollution and extremely severe regional haze episodes across the country, more efforts in air pollution control are or will be required. Since 2010, selective catalyst reduction (SCR) systems have been widely applied in power sector for NO_x control, and a set of emission standards across various sectors, have been updated or proposed, with much more tightened criteria pollutant emission limits than previous ones. The announcement of national plan of air pollution control action is expected to result in further solid work on emission abatement and air quality improvement in the future (Zhao et al., 2014).

Although not specific for Hg control, those above-mentioned policy and measures have ancillary benefits of atmospheric Hg emission abatement. For example, the use of advanced dust collectors (e.g., fabric filter (FF) and electrostatic precipitator (ESP)) and FGD are expected to capture part of Hg into fly ash or gypsum and to significantly reduce the emission levels (USEPA, 2002a; Wang et al., 2010b). SCR catalyst is able to convert part of Hg^0 to Hg^{2+} that is more liable to be absorbed by the FGD scrubber (Wang et al., 2012; Tian et al., 2012). The varied penetrations of air pollutant control devices are confirmed to be effective in global Hg emission trends (Streets et al., 2009a) and thereby the deposition patterns through simulation (Corbitt et al., 2012). From 2005 to 2010, the China's FGD penetration in power sector increased from 13 to 86 % of total capacity (Zhao et al., 2008, 2013), and the SCR penetration is ex-

ACPD
14, 26803–26855, 2014

pected to reach 70 % in 2015 from 10 % in 2010 (Wang, 2013). If such swift changes of emission control are not well evaluated, possible overestimate in recent and future emissions for the country would be made, and misleading conclusions (e.g., elevated contribution of China's emissions to the Hg pollution) would be drawn once those estimates are further used for model simulation. Besides the recent and future trends, the uncertainty of Hg emissions is not thoroughly analyzed, which is another big concern in the community (Pacyna et al., 2010; Ci et al., 2012). Till now only the uncertainty of emissions from power sector are systematically quantified for the country (Wu et al., 2010), attributed mainly to the limited information of other emission sources. The lack of analysis on emission control effectiveness and uncertainty in emissions might lead to inconsistence between the estimated increased emissions (driven by Asia) and decreased worldwide trends in background atmospheric Hg concentrations (Slemr et al., 2011; Ci et al., 2012).

This study, therefore, evaluates the effects of recently implemented and ongoing control measures on the past and future inter-annual trends and sector distributions of China's anthropogenic Hg emissions. The uncertainty of emissions is quantified with most sensitive parameters identified for further improvement of emission estimate. Section 2 briefly describes the methodology of emission inventory development with improved data and methods for certain emission sources specifically stressed, the basic assumptions in scenarios for future emission prediction, and the Monte-Carlo framework of uncertainty analysis. Section 3 is a thorough analysis of Hg emission factors by species, sector and year, incorporating the latest information of emission control strategies and the data of domestic field measurements and investigations. Section 4 presents China's recent trends of anthropogenic Hg emissions (2005–2012) and future trajectories by scenario (till 2030), the effects of pollution control measures, evaluation of emissions against other studies, and the uncertainties of emissions with main sources. Section 5 summarizes the present study.

ACPD
14, 26803–26855, 2014

2 Methodology and data sources

2.1 Brief summary of Hg emission estimate

The research domain covers the 31 provinces of mainland China, and annual Hg emissions with speciation (Hg^0, Hg^{2+}, and Hg^p) at provincial level are estimated from 2005 to 2012 to evaluate the effectiveness of China's air pollution control measures. Main anthropogenic activities fall into three main sector categories: coal-fired power plants (CPP), all other industry (IND), and the residential and commercial sector (RES). IND is further divided into cement production (CEM), iron and steel plants (ISP), heating boilers (HB), other industrial boilers (OIB), nonferrous metal smelting (NMS), gold metallurgy (GM), and other miscellaneous processes (OMP). RES mainly includes the coal combustion (RC), oil and gas combustion (ROG), biofuel use/biomass open burning (BIO), and solid waste incineration (SWI) subcategories. As the dominating primary energy resource, coal plays important roles in China's anthropogenic pollutant emissions (Zhao et al., 2013). In this work, therefore, the Hg emissions from coal use are estimated based on the above-mentioned source categories, e.g., power plants, industrial boilers, residential coal stoves, and iron and steel production (most emissions of which come from coal use). For cement production, Hg emissions come both from coal combustion and non-combustion process, and a new method is developed in this work to differentiate the two parts, as described in Sect. 2.2.

In general, annual emissions of total and certain speciation Hg for a given province i and a given year t are calculated using Eqs. (1) and (2), respectively:

$$E_{i,t} = \sum_m \sum_n \mathrm{AL}_{m,n,i,t} \times \mathrm{EF}_{m,n,i,t} \tag{1}$$

$$E_{i,t,s} = \sum_m \sum_n \mathrm{AL}_{m,n,i,t} \times \mathrm{EF}_{m,n,i,t} \times f_{m,n} \tag{2}$$

where E is the Hg emission; AL is the activity levels (fuel consumption or industrial production), EF is the combined emission factor (emissions per unit of activity level);

Discussion Paper | Discussion Paper | Discussion Paper | Discussion Paper |

ACPD

14, 26803–26855, 2014

The effects of China's pollution control on atmospheric Hg emissions

Y. Zhao et al.

f is the mass fraction of given Hg speciation; i, t, m, n and s represent province, year, emission source type, technology of manufacturing and emission control, and Hg speciation (Hg^0, Hg^{2+} or Hg^p).

For coal combustion, Eq. (1) can be further revised to Eq. (3) with detailed combustor and fuel information:

$$E_{i,t} = \sum_m \sum_n \mathrm{AL}_{m,n,i,t} \times \mathrm{HgC}_{i,t} \times R_{m,n} \times \left(1 - \eta_{m,n,t}\right) \quad (3)$$

where HgC is the Hg content of coal by province; R is the mass fraction of Hg released from fuels; η is Hg removal efficiency of air pollution control devices.

There are some sources of which the emissions cannot be directly calculated based on emission factor and activity level, attributed mainly to lack of information. Artisanal and small-scale gold metallurgy (ASGM), for example, was officially prohibited in 1990s, but it may still exist illegally in some areas driven by huge economic profit. Difficult to estimate the penetration of those technologies, the results of expert judgment have to be applied in this work (AMAP and UNEP, 2013).

Activity levels for 2005–2012 are compiled annually by sector from various data sources. Multiple-year fossil fuel consumption and industrial production at provincial level are obtained from Chinese official energy (NBS, 2013a) and industrial economy statistics (NBS, 2013b), respectively. The coal consumptions from CEM and ISP are calculated following the methods by Zhao et al. (2011, 2012), and the coal consumption by OIB is estimated by subtracting the fuel consumed by CEM, ISP and HB from that by IND (Zhao et al., 2012). The annual biofuel use before 2008 are taken from official statistics (NBS, 2013a), and those for the following years are from unpublished data by Ministry of Agriculture, since official statistics stopped reporting the relevant data from 2008 (C. Chen et al., 2013). The biomass combusted in open fields are calculated as a product of grain production, waste-to-grain ratio, and the percentage of residual material burned in the field, as described in Zhao et al. (2011, 2012). The urban municipal waste burned are taken from statistics (NBS, 2013c), and rural ones are calculated as

ACPD
14, 26803–26855, 2014

a product of rural population, the average waste per capita, and the ratios of waste that is burned (Yao et al., 2009).

The Hg emission factors, speciation and the time-series trends due to improved controls will be described by sector in Sect. 3.

2.2 Improved methods of emission estimate for given sources

The data and methods of emission estimate for given industrial sources are updated in this work to better understand the effectiveness of ongoing pollution control measures in China. Those sources include cement, iron and steel production, and nonferrous metal smelting, the emissions of which were traditionally estimated with uniform and time-independent emission factors at sector average level.

With improved data on kiln technology and emission control devices (Lei et al., 2011; Zhao et al., 2013), the technology/device penetrations of cement production for multiple years are derived in this work. The Hg emission factors by control type from domestic measurements are accordingly applied to generate the inter-annual trends of emissions. Equation (3) is used as well to separate the emissions from coal use. For nonferrous metal smelting, similarly, the penetrations of different manufacturing technologies for typical years (2005, 2007 and 2010) are obtained from a plant-by-plant database developed by Tsinghua University (Wu et al., 2012), and penetrations for other years have to be interpolated attributed to lack of information. The inter-annual trends of emissions can then be estimated combining the penetration and emission factors by technology.

For iron and steel production, Hg emissions come mainly from coal-consuming processes including coking, sintering, and pig iron production. In recent years, implementation of national energy saving and pollution control policy leads to improved energy efficiency and enhanced use of emission control devices of those processes (Zhao et al., 2013). The updated information is integrated into Eq. (3) to estimate the Hg emissions for the sector by process and year. In particular, the current official statistics do not report the coal consumption for each process but the amount of coal combusted

ACPD
14, 26803–26855, 2014

as fuel and total coal use for the sector. In this work, therefore, the coal consumption by process is estimated as the combusted coal for the whole sector weighted by the process-specific energy efficiency (expressed as kg coal-equivalent per unit production, Wang et al., 2011).

2.3 Uncertainty analysis

The uncertainties of Hg emissions with different chemical speciation are quantified by sector and year using a Monte-Carlo framework developed by Zhao et al. (2011). Probability distributions are estimated for all the parameters with different principles. Ten thousands simulations are then performed to estimate the uncertainties of emissions and to identify the crucial parameters that significantly contribute to the uncertainties for different source types.

In most cases, the uncertainties of activity levels (including penetration rates of different technologies by sector) are determined following our previous work (Zhao et al., 2011, 2013). Generally, normal distributions are assumed for fuel consumption and industrial and agricultural production, with coefficients of variation (CV, the SD divided by the mean) set at 5, 10 and 20 % for power, industry and residential and commercial sectors, respectively. It should be noted that some activity levels are strongly associated with others, e.g., the use of coke, and the production of sinter, pig iron and steel. For those parameters, a correlation coefficient of 1 is applied to represent the full correlation and to avoid possible underestimate of uncertainties from the "compensation of error" mechanism (Zhao et al., 2011).

A comprehensive analysis of uncertainties of Hg emission factors was conducted by sector and species, with domestic field measurements thoroughly evaluated. For parameters with adequate measurement data, the Kolmogorov–Smirnov test for the goodness-of-fit ($p = 0.05$) is applied and bootstrap simulation is in succession conducted to determine the probability distributions if the test is passed (Frey and Zheng, 2002; Zhao et al., 2010, 2011). For parameters that fail to pass the goodness-of-fit test or those with limited observation data, probability distributions must be assumed with

ACPD
14, 26803–26855, 2014

experience of previous work (e.g., Wu et al., 2010) and authors' judgment. The details for emission factor uncertainties by sector will be discussed in Sect. 3.

For ASGM of which the emissions were not calculated with emission factor methodology but directly taken from other study, the uncertainties are assumed at ±67 % according to expert judgment (AMAP and UNEP, 2013).

2.4 Emission projections till 2030

Three scenarios are determined to predict China's atmospheric Hg emissions in 2015, 2020 and 2030. Scenario 0 (S0) is the most conservative case in which the national policy of energy saving and air pollution control will not change in practice after 2012. This does not imply, however, that the penetration levels of advanced technologies and emission control devices for specific will necessarily be the same as in 2012. For example, the current policy on power sector will undoubtedly raise the use of FGD and SCR systems, and that on cement will increase the share of precalciner kilns with FF systems (the share of precalciner kilns would reach 100 % in 2030, compared to 88 % in 2012). While keeping the control strategy the same as S0, Scenario 1 (S1) integrates the national energy policy commitments that have been announced (e.g., the plans to reduce fossil energy use and to reduce greenhouse gas emissions) and thus shows the benefits of energy saving on Hg emissions. The activity level data for S0 and S1 come respectively from the CPS and NPS scenarios by our previous work (Zhao et al., 2014), which are mainly based on the projection by IEA (2012) with revisions on specific sectors including power and transportation. For sources that are not mentioned in Zhao et al. (2014), the specific working reports are consulted. For example, the burned ratio of urban municipal solid waste is assumed to reach 50 % in 2030, according to CAUES (2013). Scenario 2 shares the same activity level trends as S1 but includes more stringent emission control mainly for industrial sources. Those measures include use of advanced control devices specifically for Hg removal on new-built power plants, use of FGD systems for new-built industrial and heating boilers, use of SCR for new-built cement precalciner kilns since 2020, more penetrations of electric furnaces for steel smelting resulting in less pig iron production and thereby less coal combustion, and more penetrations of advanced manufacturing technologies with lower Hg emission factors for non-ferrous metal smelting. The detailed benefits of those technologies on Hg emission control can be found in Sect. 3.

3 Evolution of emission factors

3.1 Evolution of emission factors for key sectors with key assumptions and uncertainties

The improvements of emission factors come mainly from two aspects: (1) new and better data available from domestic measurements for key sectors; and (2) better understanding on penetration variations of manufacture and control technologies for different sources during 2005–2012. Those improvements thus provide more accurate emission factors with clearer inter-annual trends by sector, as shown in Fig. 1. In this study, a comprehensive review of literatures is conducted and an updated database for China's atmospheric Hg emission factors is established, with their uncertainties carefully analyzed expressed by probability distribution functions (PDF), as summarized in Table 1.

3.1.1 Power plants

As Eq. (3) indicates, the integrated Hg emission factor for power plants, expressed as the metric tons (t) Hg emissions per million metric tons (Mt) coal combusted, are calculated as the product of the Hg content of coal, release rate of specific combustion facility and one minus Hg removal efficiency of air pollution control device (APCD).

Hg content of coal in China has been addressed by a series of studies (Wang et al., 2000; Huang and Yang, 2002; Feng et al., 2002; USGS, 2004; Zheng et al., 2006; Zhang et al., 2012a), and the method by Wu et al. (2010) is followed in this work to

Discussion Paper | Discussion Paper | Discussion Paper | Discussion Paper |

ACPD

14, 26803–26855, 2014

The effects of China's pollution control on atmospheric Hg emissions

Y. Zhao et al.

determine the values and uncertainties by province, i.e., the percentiles of Hg content by province are estimated based on the available measurements data and the lognormal distributions are conservatively applied as PDF, with relatively long tails for most provinces. Regarding the release rates, the values for of pulverized combustion (PC), circulating fluidized bed (CFB), and grate boiler reach 98.7, 98.4, and 95.9 %, respectively, indicating that most Hg in coal is emitted into the flue gas due to the high combustion temperature (see details in Table S1 in the Supplement). Since current available measurements are not sufficient for data fitting to determine the uncertainty, triangular distributions are assumed for the parameter, with 10 and 90 % percentiles as the lowest and highest investigated values from measurements, respectively.

As the main emission control target since 2005, the use of advanced APCD has increased fast in coal-fired power sector. The penetration rates of FGD and SCR systems, for example, reached 90 and 27 % respectively in 2012. Those technologies are confirmed to result in lower Hg emission factors and thereby side benefits of Hg removal (Wang et al., 2012). In this work, the removal efficiencies of major types of APCDs including ESP, FF, ESP+FGD, SCR+ESP+FGD, are analyzed combining most recent field measurements for China's power plants (see details in Table S2 in the Supplement). As shown in Fig. 2, the system of SCR+ESP+FGD has the highest Hg removal efficiency at 76.6 %, followed by FF at 56.1 % and ESP+FGD at 53.8 %. Large variations of Hg removal efficiencies of APCDs are indicated by different studies, and the values estimated and applied in this work are relatively conservative, particularly for ESP+FGD, currently the dominating APCD for power sector. In addition, the removal efficiencies are much lower than those from developed countries like US and Japan. Part of reasons could be the large difference in coal quality between countries and poorer running conditions of APCD in China (Li, 2011; Zhi et al., 2013). For other dust collectors including wet scrubber (WET) and cyclone (CYC), limited domestic information from field tests is obtained and applied in this work (e.g., Huang et al., 2004), leading to higher removal efficiencies than previous inventory work (Streets et al., 2005; Wu et al., 2006). We believe those values would not significantly enhance the uncer-

ACPD
14, 26803–26855, 2014

tainty since the capacity share of units with WET or CYC is small, e.g., at roughly 2 % in 2010. Regarding the possibility of further improvement on Hg emission control in the future, new-built power units are assumed to apply the powdered activated carbon (PAC) injection technology (Srivastava et al., 2006; Cui et al., 2011) or modified catalytic oxidation of elemental Hg (Guo et al., 2011; Yan et al., 2011) in S2, and average Hg removal efficiencies of those technologies are expected to reach 90 %. The PDF of removal efficiencies by device are estimated following the instruction described in Sect. 2.3. In most cases, the PDFs are assumed to be Weibull distribution due to insufficient data samples. For ESP, however, the data from current available measurements passed the statistical test and bootstrap simulation is applied to determine its PDF as normal distribution, as shown in Fig. 3a.

Attributed mainly to the distinctly growing use of APCD, the average Hg emission factor for power plants is estimated to decrease 0.13 in 2005 to 0.08 g (t-coal)$^{-1}$ in 2012, as shown in Fig. 1a. With PAC injection applied in S2 in the future, the average emission factor would further decrease to 0.05 g (t-coal)$^{-1}$ in 2030.

3.1.2 Iron and steel production

In previous studies, a uniform emission factor of 0.04 g (t-steel)$^{-1}$ is generally applied for iron and steel production, with little consideration of technology improvement (Streets et al., 2005; Wu et al., 2006). In this work, as described in Sect. 2.2, latest information on APCD penetration trends and removal efficiencies is combined and Hg emissions are calculated separately for each coal-consuming process with Eq. (3), and then aggregated to the sector level. The Hg release ratios of coking and pig iron production are estimated at 63 and 84 %, respectively (Wang et al., 2000; Hong et al., 2004), with uniform distributions conservatively determined for lack of updated results from measurements. Without specific information, the removal efficiencies with PDF for iron and steel industry are assumed to be the same as those for power sector. Such assumption is expected to result in possible underestimate of emissions for the sector, since the APCD operations might not be as good as those for power plants. Although

ACPD
14, 26803–26855, 2014

that possible underestimate could be partly quantified by uncertainty analysis, more investigation on APCD benefits on Hg removal for sectors other than power plants are further needed.

Driven by the increased penetration of advanced manufacturing and emission control technologies, in particular, the growth of machinery coking, the emission factor is estimated to have declined from 0.071 to 0.039 g (t-steel)$^{-1}$ from 2005 to 2012, indicating that the application of 0.04 g (t-steel)$^{-1}$ might underestimate the emissions for the sector previous years (Fig. 1b). Regarding the future projection, the ratio of pig iron to steel is assumed to decrease from 92 % in 2012 to 80 % in the S2, 2030, due to expanding use of electric arc furnaces that apply more waste steel inputs instead of more energy-intensive inputs including pig iron (Wang et al., 2007; Zhao et al., 2012). The emission factor would thus further reduce to 0.035 g (t-steel)$^{-1}$.

3.1.3 Non-ferrous metal smelting

Although non-ferrous metal industry including Pb, Zn and Cu smelting is estimated as one of the main sources of Hg emissions (Li et al., 2010; Wu et al., 2012), the available emission factors from field tests are still limited, given the multiple and complex factors that are influential in emission levels (e.g., the Hg concentration in ore concentrate, smelting technology, the penetration of acid plants and APCDs). Based on those limited data, a process-based methodology is developed and applied in this work to estimate the emission factors for various kinds of smelters employed in China, as shown in Table S3 in the Supplement. All the processes and their corresponding emission factors are obtained from field measurements (Feng et al., 2004; G. Li et al., 2009; Li et al., 2010; Wang et al., 2010; Zhang et al., 2012b) or field-based calculation (Wu et al., 2012). In particular, oxygen pressure leaching process for Zinc smelting has not been included in the table, because it does not include the process of high temperature calcination and thus little mercury is released to the atmosphere. Given the very small sample size, uniform distribution has to be assumed for most cases, with 10th and

90th percentiles set as the minimum and maximum values from field measurements, respectively.

Based on the plant-by-plant database (Wu et al., 2012) and the name list of small smelters that have been shut down since 2010, the penetrations of various kinds of smelters are calculated by year and non-ferrous metal type, and the inter-annual trends of emission factors can then be analyzed. As shown in Fig. 1d–f, the national average EFs for Zn, Pb and Cu smelting are estimated to drop from 15.5, 16.7, and 1.7 g (t-product)$^{-1}$ in 2005 to 13.3, 4.7, and 0.2 g t^{-1} in 2012, respectively. In S2 for future projection, the EFs are predicted based on the assumption that the most advanced technologies will compulsorily be applied for the new-built smelters. The EFs for Zn and Pb are thus estimated to further reduce to 9.1 and 2.2 g (t-product)$^{-1}$ in 2030, respectively.

3.1.4 Cement production

Series of studies have been conducted to measure the Hg emission levels of cement production (Li, 2011; Zhang, 2007). Based on the available data from those field tests the emission factors are estimated at 0.008, 0.052 and 0.120 g (t-product)$^{-1}$ for cement kilns with FF, ESP, and WET dust collectors, respectively. The data sample for FF passed the statistical test and bootstrap simulation is applied to determine its PDF as Weibull distribution, as shown in Fig. 3b. For other dust collectors, however, the current data are limited and uniform distribution are used, with 10th and 90th percentiles set as the minimum and maximum values from field measurements, respectively.

Combining the inter-annual trends of APCD penetration for the sector (Lei et al., 2011; Zhao et al., 2013), the national average of emission factor is estimated to decline from 0.06 in 2005 to 0.018 g t^{-1} in 2012 (Fig. 1c), resulting mainly from the sharp increase of precalciner kilns with FF. For the future, all the kilns other than precalciner are estimated to be shut down since 2020 for S1 and S2, and 2030 for all the scenarios, and SCR systems will be used for precalciner kilns in S2 (Zhao et al., 2014). Those improvements would lead to the sector-average EF reduced to 0.013, 0.012 and

0.008 g (t-product)$^{-1}$ for S0, S1 and S2 in 2030, respectively. Regarding the emissions from coal combustion in cement production, the Hg removal efficiencies for various APCDs are applied to generate the emission factors, and the national average value is estimated to be reduced from 0.11 to 0.08 g (t-coal)$^{-1}$ during 2005–2012. While no significant abatement is found for S0 and S1 after 2010, the emission factor would further decrease to 0.04 g (t-coal)$^{-1}$ for S2, 2030, attributed to the growth of SCR application in the scenario.

3.1.5 Other industrial sources

Emission factors of industrial and heating boilers are estimated using Eq. (3). The Hg release ratios for grate boilers and CFB are estimated at 76 and 91 % based on limited domestic measurements (Wang et al., 2000; Tang et al., 2004), lower than those for power plants. Uniform distributions are used to quantify the uncertainty of the parameter. WET and CYC are the dominating types of dust collectors for boilers and their removal efficiencies with PDF are assumed to be the same as those for power plants. For S2 in the future, FGD are assumed to be used for the new-built boilers, leading to larger fraction of Hg removal.

Production of polyvinyl chloride polymer (PVC) is a significant contributor to the Hg emission due to the widely using of mercuric chloride catalyst in the acetylene technologies. The emission factor is calculated as the product of Hg content in PVC and its release ratio to atmosphere during the production process. In this work, the Hg content in PVC is estimated to range 0.12–0.20 kg Hg (t-PVC)$^{-1}$ based on investigation by Hao et al. (2005) and the release ratio at 1 % according to THU (2009). For other processes including Hg mining, production of battery and fluorescent lamp, large-scale gold production, and oil/gas combustion, the emission factors from AP-42 (USEPA, 2002a) and previous inventory work (Streets et al., 2005) are used due to lack of updated information from domestic measurements, and lognormal distributions are assumed with CV conservatively set at 100 %.

ACPD
14, 26803–26855, 2014

3.1.6 Residential sources

For residential coal consumption, the determination of Hg emission factors is similar as that for industrial boilers. Biomass combustion in this work includes crop residue (used as biofuel in household and as waste burned in open fields) and fuel wood (used for household). Domestic information and field measurements (Huang et al., 2011; Zhang et al., 2013) are adopted in this work to estimate the emission factors, and uniform distributions are assumed reflecting the relatively big uncertainty. Based on domestic dataset, the average EFs for crop residue (16.7 $ng\,g^{-1}$) and fuel wood (12.3 $ng\,g^{-1}$) calculated in this work are lower than the values adopted in previous study (e.g., 37 $ng\,g^{-1}$ for crop residues and 20 $ng\,g^{-1}$ for fuel wood, Streets et al., 2005).

Hg emissions from solid waste incineration (SWI) are estimated separately for municipal solid waste incineration (MSWI) and rural household waste incineration (RHWI) due to the different mercury content levels and burning methodologies. For MSWI, an emission factor of 0.22 $g\,t^{-1}$ with Weibull distribution is evaluated with bootstrap simulation based on domestic field tests by L. Chen et al. (2013) and Hu et al. (2012) (Fig. 3c). The emission factor for RHWI is estimated as the product of Hg content and release ratio to atmosphere, which are obtained from Hu et al. (2012).

3.2 Speciation of Hg with probability distribution functions

Besides the total amount, the speciation of Hg emissions plays a crucial role in understanding the transport and cycling of Hg since the activity of Hg depends significantly on the chemical form. The fate of Hg (Hg^0, Hg^{2+}, and Hg^p) released to atmosphere can be primarily affected by the fuel quality and the removal mechanisms of APCDs, and thereby varies largely among different emission sources. In this work, a thorough investigation on existing studies is conducted to compile a database of Hg speciation by sector and thus to provide the mass fractions of the three chemical forms of Hg (see details in Table S4 in the Supplement). In general, the emission sources for determination of Hg speciation can be divided into three categories according to APCD

Discussion Paper | Discussion Paper | Discussion Paper | Discussion Paper |

ACPD

14, 26803–26855, 2014

The effects of China's pollution control on atmospheric Hg emissions

Y. Zhao et al.

application and data availability. In the first case, for sources whose emission factors are calculated with the removal efficiencies of different APCD considered (e.g., CPP, CEM, ISP, OIB and RC), the mass fractions are estimated based on the results from field measurements by APCD type. The second, for sources lack of sufficient measurement sample to determine emission factors by APCD type, the average values of available field test results are calculated and applied as mass fraction of speciation for the sector (e.g., NMS, BIO and SWI). The third, for sources that very little domestic information can be found in speciation split, results from global studies (Pacyna and Pacyna, 2002) have to be used and little update is made compared to previous inventory work (Streets et al., 2005). Those sources mainly include industrial processes like artisanal gold production, Hg mining, battery and fluorescent lamp production, etc.

As shown in Table S4, the speciation split of total Hg varies largely among different types of APCD combination. For example, the average of Hg^0 mass fraction reaches 83 % for FGD+ESP, attributed to the relatively strong removal effects of the both APCDs on Hg^{2+} and Hg^p. Once SCR applied, significant increase of Hg^{2+} fraction is observed, resulting mainly from the conversion of Hg^0 to Hg^{2+} by SCR (Wang et al., 2010b). In general, oxidation of Hg^0 leads to higher removal of Hg since Hg^{2+} is more liable to be adsorbed, and use of advanced dust collectors leads to lower Hg^p as most of them can be captured with particles.

For mass fraction data that pass the Kolmogorov–Smirnov test, bootstrap simulation is applied to determine their PDF, e.g., the mass fractions of Hg^{2+} for ESP, ESP+FGD and SCR+ESP+FGD (Fig. 3d–f). Otherwise, triangular or uniform distributions are applied. The PDFs for Hg speciation are summarized in Table 2.

ACPD
14, 26803–26855, 2014

4 Results and discussion

4.1 Historical trends in mercury emissions to the atmosphere

The national total emissions of anthropogenic Hg are estimated to increase from 679.0 metric tons (t) in 2005 to 749.8 t in 2012, with the peak at 770.6 t in 2011, as shown in Fig. 4. The annual growth rate of emissions can then be calculated at 2.1 % during 2005–2011, much lower than that of energy consumption (7.6 %) or economy of the country (> 10 %). Although slight increase in emissions is evaluated for recent years, the inter-annual variation is much smaller than the estimated uncertainty of annual emissions (provided in Sect. 4.4). That indicates the constrained Hg emissions for the country since 2005, compared to relatively fast growth in early 2000s (e.g., 8 % of annual growth of Hg emissions suggested by Wu et al., 2006 from 2000 to 2003). This trend, however, is currently difficult to be confirmed through field observations of atmospheric ambient Hg in China, attributed mainly to lack of middle and long term Hg observation, either in polluted cities or background areas. Limited inter-annual results for background areas (Changbai Mountain in northeastern China) show reduced Hg levels (Wan et al., 2009; Fu et al., 2012b). Those differences, however, are believed to come from changes in sampling location instead of in emissions (personal communication with X. Fu from Institute of Geochemistry Chinese Academy of Sciences, 2014). Tightened air pollution control in China, even not specifically for Hg, should be important reasons for the smooth emission trends, and it will be interpreted in details in Sect. 4.2. The speciation of Hg emissions is relatively stable for recent years, with the mass fractions of around 55, 39 and 6 % for Hg^0, Hg^{2+} and Hg^p, respectively.

The annual emissions by sector are summarized in Table 3. Coal combustion, gold metallurgy and nonferrous metal smelting are the most significant Hg sources of anthropogenic origin, accounting together for 85 % of national total emissions. Coal combustion from power sector, industrial and heating boilers, cement kilns, residential stoves and iron and steel production, is the largest contributor to Hg emissions, and its share to national total emissions is estimated to increase from 43 % in 2005 to 49 %

ACPD
14, 26803–26855, 2014

in 2012. This is mainly because the relatively constant emission levels are evaluated for gold metallurgy and nonferrous metal smelting sectors during the same period, resulting from penetrations of newer and more advanced manufacturing technologies under the national policy of emission control. Emissions of Hg^0, Hg^{2+} and Hg^p are summarized by sector in Tables S5–S7 of the Supplement. For Hg^0 and Hg^{2+}, the three biggest sources are the same as those for total Hg emissions, i.e., coal combustion, gold metallurgy and nonferrous metal smelting. For Hg^p, coal combustion plays a dominant role to the emissions, with the share ranged 78–84 % for various years, since very few Hg^p emissions are assumed from gold metallurgy, zinc and lead smelting in this work.

Provincial emissions with inter-annual variability are analyzed and illustrated in Fig. 5. Attributed to unclear amount and spatial distribution, Hg emissions from ASGM are not included in the provincial analysis. While coal combustion is identified as the biggest source of atmospheric Hg for most provinces, relatively high emissions from non-combustion sources are estimated for several provinces including Hunan, Yunnan, Henan, Guangxi, Anhui, and Shaanxi, resulting mainly from the large production of Zn and/or Pb in those regions. Clear difference in emission trends from 2005 to 2012 is found by region. In contrast to most provinces that have had their emissions increased, reduced emissions are prominently estimated for the three regions with largest density of population, economy and pollution in China, i.e., Jing-Jin-Ji region (JJJ, including Beijing, Tianjin and Hebei), Yangtze River Delta region (YRD, including Shanghai, Jiangsu and Zhejiang), and Pearl River Delta region (PRD, including Guangdong). The share in Hg emissions of those 7 provinces is estimated to decline from 24 % in 2005 to 19 % in 2012, similar with other criterion air pollutants (Zhao et al., 2013). This deviation in emission trends, on one hand, indicates the slower increase in industry with heavy pollution and the progress of emission control in developed regions. On the other hand, however, it reveals that China's air pollution challenges have been expanding to less developed interior provinces, resulting from rapid urbanization, accelerated economic development, and fast growth of pollution sources in those areas.

ACPD
14, 26803–26855, 2014

4.2 Implication of emission control on national Hg emissions

Instead of keeping fast increasing driven by the accelerated economic growth, China's Hg emissions of anthropogenic origin have been efficiently restrained since 2005, indicating the success of national strategies on the Hg emission control. Contributing together to this apparent national trend, the emission trends by sector, however, vary greatly attributing to different driven factors and uneven control policies. Detailed analysis is thus conducted to explore the sources dominating the Hg emission trends. Due to lack of accurate information, high uncertainty exists in the estimation of emissions from ASGM, and its annual emission level is unchanged over-time in this work. Although recognized as the biggest contributor to total Hg emissions among all the single sources (Table 3), ASGM is not included here as a type of source that has direct effects on the national emission trend.

Therefore, we divide the rest anthropogenic sources into three categories, as indicated in Fig. 6a. The first category includes sectors for which uniform and unchanged emission factors are applied through the sector over-time (i.e., OMP, BIO, SWI and large scale gold metallurgy). The inter-annual variability of Hg emissions from those sources are thereby only affected by the changes of activity levels, and the annual emissions for category-1 sectors have been keeping increasing from 80.3 in 2005 to 109.8 t in 2012. Due to their relatively small fraction to the total anthropogenic emissions (< 15 %), however, the category-1 sectors have little influence on the trend of national total emissions that shows much slower growth with even declined emissions for a few years, as shown in Fig. 6a. The second category consists of coal combustion for heating (HB), other industrial boilers (OIB) and residential use (RC and ROG), for which the emission factors are region-dependent, with little inter-annual variation due to very limited pollution control measures implemented. Hg emission trend of those sources, therefore, depends mainly on the intensive coal use for the recent years, and the emissions in 2012 are estimated 47 % lager than 2005. The third category includes coal-fired power plants (CPP), cement production (CEM), iron and steel plants (ISP)

ACPD
14, 26803–26855, 2014

and nonferrous metal smelting (NMS). Although the activity levels (i.e., coal consumption and industrial production) increased for those sources similar as category-1 and -2 sectors, Hg emission trends of category-3 sectors are dominated by the co-effects of emission control on criteria air pollutants through increased use of APCD and improved manufacturing technologies. The emissions of the sectors are estimated to reach peak at 362 t in 2007 and then to be reduced to 313 t in 2012, largely offsetting the increase in emissions from the above two categories and playing a crucial role in constraining the national total emissions.

Figure 6b compares the trends of activity levels and Hg emissions for category-3 sectors from 2005 to 2012. During the period, coal consumption of coal-fired power plants, cement production, steel production and nonferrous metal production increased by 70, 107, 158 and 104 % respectively. A leveling off in 2008 was found for industrial production, attributed mainly to the production limitation imposed for the Beijing Olympics and to the economic recession at the end of 2008. However, the economy activities increased sharply again under a major economic stimulus policy to respond to the recession, and the energy and industrial production keep fast growing in the following years. In contrast to the large growth of activity levels, the Hg emissions from the four sectors are clearly constrained to varying degrees: those from CEM decreased by 38 %, those from CPP and NMS in 2012 dropped to the levels in 2005, and those from ISP increased by 44 %, far less than growth of steel production. As described in Sect. 3, the reduced emission factors through the period are the main reasons for the emission abatement, attributed to the replacement of old and small plants or kilns with those with advanced control technologies and high combustion efficiencies. The increased penetrations of FGD and SCR in CPP, precalciner kilns with FF in CEM, machinery coking with ESP in coking, and improved manufacturing technologies in NMS have lead to great ancillary benefits of atmospheric Hg emission abatement. As indicated in Fig. 7, the implemented emission controls are estimated to cut 100, 93, 30 and 76 t of Hg emissions in 2012 for CPP, CEM, ISP and NMS, respectively, compared to a hypothetic case in which no progress of emission control is assumed for the four sec-

ACPD
14, 26803–26855, 2014

tors since 2005. Without the controls, the Hg emissions of those sectors in 2012 would then exceed 600 t, almost doubling the current estimate. It can thus be confirmed that China's pollution controls in power and certain industrial sectors have greatly slowed down the national Hg emissions.

4.3 Evaluation on reliability of the estimated emissions against other studies

The estimated China's total Hg emissions in this work can hardly be compared directly with other studies for two main reasons: (1) very few studies were conducted on China's national total Hg emissions for continuous years after 2005, the period with dramatic changes in emission controls across the country; and (2) the sectors and sources of anthropogenic Hg emissions concerned are not completely the same between different emission inventories. Wu et al. (2006) estimated China's Hg emissions at 696 t in 2003, slightly larger than our estimate for 2005. Given the fast growth of economy and energy use for the following years, our study thus yields lower estimates for China's Hg emissions once the benefits of emission controls are included in the analysis. This revision is supported by chemistry simulation that overestimated the ambient Hg concentrations based on previous inventory studies (personal communication with H. Zhang from Institute of Geochemistry Chinese Academy of Sciences, and L. Wang from Tsinghua University, 2014). A more recent study evaluated the emissions of China's anthropogenic Hg at 643 t for 2007, roughly 100 t smaller than our estimate (Wang et al., 2014). Compared with observations, however, lower levels of ambient total Hg or Hg^0 were generally simulated through GEOS-Chem based on the calculated emissions for background/rural sites, indicating a possible underestimate of Hg emissions (Wang et al., 2014). The results of speciation analysis are similar between Wu et al. (2006) and this work, with slightly larger mass fraction of Hg^p (12 vs. 6 %) but smaller for Hg^{2+} (32 vs. 39 %) by Wu et al. This is probably attributed to oxidation of Hg^0 by APCDs and increased use of advanced dust collectors after 2005. Besides the total emissions, clear differences exist between studies by sector, motivating the analysis on certain sources of atmospheric Hg emissions.

ACPD
14, 26803–26855, 2014

For coal combustion sources as a whole, Tian et al. (2010) calculated the Hg emissions at 284 and 306 t for 2005 and 2007, respectively, close to our estimate. In particular, Hg emissions from CPP during 2005–2010 have been evaluated by several studies. Streets et al. (2009b) calculated the emissions for 2005 at 125 t, while Tian et al. (2012) estimated the annual emissions during 2005–2007 ranged 135–139 t, with little inter-annual variability. Those estimates are somewhat lower than our results. Although the differences could be attributed to many factors including discrepancies in depth of details in boiler technologies and data sources of Hg content in coals, the conservative removal efficiencies of APCDs for Hg evaluated and applied in this work (as shown in Fig. 2) are believed to be the most important reason responsible for the higher estimate of Hg emissions. Wang et al. (2010c) estimated that Hg emissions from CPP would reach 155 t in 2010, larger than our results. However, the energy data and penetrations of APCDs (especially FGD) in Wang et al. (2010c) were not from actual statistics but prediction based on Zhao et al. (2008), as the actual data for 2010 were unavailable when the study was conducted. The larger annual coal consumption by CPP (1735 million metric tons in the study vs. 1576 in actual facts) and lower penetrations of FGD (70 % in the study vs. 86 % in actual facts) than the actual facts would lead to a possible overestimate of Hg emissions for the sector. Compared with all those studies, therefore, the relatively low emissions of national total Hg in this work could probably not be attributed to underestimate of emissions from CPP but to improved estimates for certain other sources as described below.

For NMS, constant emission factors were commonly used in previous inventories attributed to lack of detailed analysis on the trends of manufacturing technology penetrations and thereby the synergic effects of Hg emission mitigation. Feng et al. (2009) evaluated that the emission factors of NMS in China could reach 155 g (t-Zn)$^{-1}$, 44 g (t-Pb)$^{-1}$, and 10 g (t-Cu)$^{-1}$ by summarizing the results from previous studies, while Pirrone et al. (2010) adopted 7 g (t-Zn)$^{-1}$, 3 g (t-Pb)$^{-1}$, and 5 g (t-Cu)$^{-1}$, based on the results from developed countries, to estimate the China's emissions in 2003. If those two datasets were applied without consideration of possible variability through years,

ACPD
14, 26803–26855, 2014

Hg emissions from NPS in 2012 would then be calculated at 672 and 80 t, i.e., 635 % larger and 12 % lower than this work, respectively. The big gaps between different studies, as indicated in Fig. 8a, reveal the importance of better tracking the inter-annual trends of emission factors for the sector. Based on a detailed survey on individual smelting plants, a more recent study by Wu et al. (2012) developed a technology-based methodology with consideration of smelting processes, mercury concentration in concentrates, and mercury removal efficiencies APCDs. They calculated the emissions declining from 87 in 2005 to 72 t in 2010, more consistent with our study than those using constant emission factors.

For ISP and CEM, emission factors in previous inventories were mainly obtained from Pacyna and Pacyna (2002) and Streets et al. (2005), respectively, i.e., 0.04 g (t-product)$^{-1}$. With these uniform emission factors adopted, Hg emissions from the two sectors during 2005–2012 would be evaluated to keep increasing from 15 to 38 and 43 to 88 t, respectively, as shown in Fig. 8b and c. This would definitely ignore the effects of improved manufacturing technologies and increased use of APCDs on emission growth constraint, and would potentially overestimate the emissions particularly for the most recent years. For MSWI, the emission factor of 2.8 g t^{-1} from UNECE/EMEP (2004) was widely accepted in previous inventories. Series of domestic field measurements, however, suggested a much smaller values of 0.22 g t^{-1} for China (L. Chen et al., 2013; Hu et al., 2012), and lower emissions are estimated in this work (Fig. 8d). Given the swift growth of solid wastes for the country, more field tests on both municipal and rural solid waste burning plants are thus imperative to confirm the levels of emission factors and to reduce the uncertainty of Hg emission estimate.

4.4 Uncertainties of national emission inventory

The uncertainties of anthropogenic Hg emissions in China for 2005–2012 are quantified with Monte-Carlo simulation and the results for selected years are summarized in Table 4. In 2010, for example, the uncertainties of total Hg emissions and those from coal combustion are estimated at −23 ~ +51 % (95 % confidence interval, CI) and

ACPD
14, 26803–26855, 2014

−49 ∼ +69 % (95 % CI), respectively. Since the annual emissions with uncertainties from ASGM are assumed unchanged during the period and thus bear large subjectivity, the uncertainties of anthropogenic Hg emissions without ASGM is further calculated at −23 ∼ +61 % (95 % CI). The uncertainties of current Hg emission inventory are believed to be partly responsible for the difference in ambient Hg levels from observation and model simulation (e.g., 0–50 % difference suggested by Wang et al., 2014). Larger uncertainties are found for Hg species than total Hg, e.g., the uncertainties of Hg^0, Hg^{2+} and Hg^p are evaluated at −31 ∼ +58, −32 ∼ +69 %, and −51 ∼ +114 % (95 % CIs) for 2010, respectively (not shown in the table). Among the three sectors (CPP, IND, and RES), the uncertainties of IND are relatively small. However, it does not imply that the emission characteristics of IND are well understood but results from the aggregation of the uncertainties of all industrial sources and thus cannot reflect larger uncertainties for certain sources.

Figure 9 illustrates the emission uncertainties by source for different Hg species in 2010. For all species, biomass burning (BIO), solid waste incineration (SWI) and residential oil and gas burning (ROG) are the sources with the largest estimated relative variations to central estimate (i.e., 95 % CIs expressed in percentages), attributed to limited field measurements on those sources. Nevertheless, some certain industrial sources, even with less relative variations, are identified as well to be crucial to uncertainties of national Hg emissions, because of their large fractions to total emissions. Those sources include coal-fired power plants (CPP) for Hg^0, nonferrous metal smelting (NMS) and gold metallurgy (GM) for Hg^0 and Hg^{2+}, and industrial and residential coal burning (OIB and RC) for Hg^p.

Table 5 summarizes the parameters that are most significant in determining the uncertainties of emissions according to their contribution to the variance of emissions. In most cases, parameters related with emission factors contribute most to the uncertainties, including Hg contents in coals for provinces with large consumption (Shandong and Henan, etc.), emission factors of biomass burning and certain technologies for nonferrous metal smelting, and removal efficiencies of dominating APCD. The amount of burned coal and biomass are found important specifically for emissions of residential sector. For Hg speciation, the mass fractions of different species for various APCDs and gold metallurgy are identified as key parameters to the bigger uncertainties than total Hg, implying the necessity of further domestic studies.

Attributed to inclusion of more results of recent measurements on emission factors, uncertainty of CPP for 2005 quantified in this work was lower than that for 2003 by Wu et al. (2003), expressed as 80 % CI. It can be seen from Table 4, however, that the uncertainties of emissions from CPP increased from 2005 to 2012. This results mainly from the fast increased penetration of FGD systems after 2005 and that of SCR after 2010, of which the co-effects of Hg control varied significantly among measured plants. In past years, the installed FGD systems are not believed to be fully operated for running cost saving, and big discrepancies in SO_2 removal efficiencies exist across the country (Xu, 2011; Zhao et al., 2013, 2014). The unclear operation of FGD leads to big ranges of Hg removal efficiencies of the systems and thus enhances the uncertainties of emission estimate, as FGD gradually dominates the sector. Besides, the Hg removal effects of SCR are still poorly quantified, and the uncertainties of Hg emissions are further elevated for most recent years since China is currently undergoing the NO_x control through broad use of SCR (Zhao et al., 2014). As shown in Fig. 10, the contribution of Hg removal efficiency of FGD to variance of CPP emissions increased from 0 % in 2005 to 26 % in 2010, and it has been the most important parameter contributing to the uncertainty of CPP emissions since 2009. In 2012, Hg removal efficiencies of FGD and SCR are estimated to contribute together 37 % of the uncertainty of Hg emissions.

The emission uncertainties of given industrial sources increased recently for similar reasons. The uncertainty of Hg emissions from NMS, for example, increased from $-46 \sim +116$ % in 2005 to $-45 \sim +169$ % in 2012. It is attributed mainly to the increase use of electrolytic process for Zinc smelting, for which the domestic measurements are rare and the emission factor bears large uncertainty. Moreover, the theoretically reduced but actually unconfirmed ratios of gold extraction by amalgamation enhance the Hg emission uncertainty of gold metallurgy. In general, therefore, the uncertainty of

ACPD
14, 26803–26855, 2014

Hg emissions increase for most recent years and possibly near future, and more field tests or investigations on certain sectors are in urgent need for better understanding the evolution of emission sources and its benefits on Hg control.

4.5 Future emission trends by scenarios

The projected national emissions through 2030 are summarized by sector in Table 6. As shown in Fig. 4 and Table 6, China's Hg emissions of anthropogenic origin are estimated to increase smoothly in the future, even with few improvements on measures specific for Hg control, as S0 and S1 in this work. The emissions in 2030 for the two scenarios are estimated at 869 and 813 t, i.e., 16 and 8 % higher than 2012, respectively. The growth in Hg emissions is far slower than that in economy and energy consumption predicted (IEA, 2012). This results mainly from the benefits of ongoing air pollution control policies in the country, such as the national action plans of air pollution prevention and control (Zhao et al., 2014). The measures of the policies will ensure continuous increase in application of advanced technologies with improved energy efficiencies and removal rates of air pollutants across various economic sectors. The national Hg emissions would then be effectively restrained through the ancillary benefits of Hg removal of those technologies. The results clearly revealed that projection of China's Hg trajectory simply based on economy/energy growth would be liable to cause overestimate.

Comparing the three scenarios, much bigger reduction in Hg emissions is expected between S0 and S2 than that between S0 and S1. The result indicates that implementation of emission controls specific for Hg is more efficient to reduce Hg than the energy conservation. In particular, if certain industrial sources like ASGM could be faithfully controlled under the national regulations (two thirds of emissions are assumed to be cut in S2 of this wok, according to the estimate by Feng et al., 2009), the national Hg emissions since 2015 would be less than that in 2005, and 23 % reduction of annual emissions can be expected in 2030 compared to 2012, with the total emissions below 600 t. For other industrial sources other than metallurgy, however, the Hg abatement in S2 is relatively limited, implying small potential of APCDs' co-effects on Hg control due to near saturated use of APCDs for various sources. Expansion of devices specific for Hg removal from power sector and manufacturing technologies in which less Hg is involved is thus essential to further reduce Hg emissions in the future. In addition, very few policies would be conducted on residential sources, resulting in elevated emissions and contribution of the sector to national total emissions. For example, the share of RES to total anthropogenic Hg emissions in S2, 2030 is predicted to reach 19 from 11 % in 2012.

5 Conclusions

Facing big challenges of severe urban and regional air pollution from swift economy development and enormous energy consumption, China has been implementing a series of policies in energy conservation and emission control since 2005. Although not specific for Hg, a pollutant with broad international interest, the policies and measures are evaluated to be effective in constraint of China's Hg emissions. From 2005 to 2012, China's atmospheric Hg emissions of anthropogenic origin are estimated to increase from 679 to 750 t, much slower than the growth of economy and energy. In particular, decreased Hg emissions are estimated for JJJ, YRD, and PRD, the regions with the largest density of population, economy and energy consumption across the country. With improved methods for emission estimate, almost half of Hg emissions are expected to be cut in 2012 together for power plant, cement production, iron and steel production and nonferrous metal smelting, attributed to the enhanced use of devices with high energy efficiencies and removal rates of pollutants after 2005. In addition, the lower emission factors through domestic measurements for biomass burning and solid waste incineration result in smaller Hg emissions than previous inventories in which global emission factors were applied. Even with considerable growth of energy predicted by IEA (2012), the continuous measures in pollution control will further restrain

ACPD
14, 26803–26855, 2014

the national Hg emission trajectory in the future. It thus indicates possible overestimate of China's Hg emissions if ongoing measures are not fully followed in the analysis.

It should be noted, however, that the uncertainties of China's Hg emission estimate are enhanced, although the slower growth of emissions seems plausible due to implementation of air pollution controls. This is mainly because of the increased use of advanced APCDs or improved manufacturing technologies for certain sectors, which are estimated to yield lower emission levels with broader uncertain ranges. Unclear operation status of APCDs and limited measurements on new technologies are the important source of uncertainty for current estimate. In addition, the unknown levels and locations of illegal ASGM contribute significantly to the uncertainty of China's Hg emissions as well. Besides the total amount, the relatively poor understanding of mass fraction of Hg speciation by sector elevates the uncertainties of emissions for different species, which are more important to atmospheric chemistry community. Given the ongoing dramatic changes of emission sources under current policies within the country, therefore, systematic investigations by sector are suggested specifically for Hg pollution, for better tracking the possible variability of emission levels, and efficiently reducing the uncertainty of emissions for all the Hg species. Middle-to-long term observations of atmospheric Hg, both in polluted urban and regional background areas, are also in great need to justify the emission analysis of China's anthropogenic Hg and to confirm the effects of implementation in pollution control in the country.

The Supplement related to this article is available online at doi:10.5194/acpd-14-26803-2014-supplement.

Acknowledgements. This work was sponsored by the Natural Science Foundation of China (41205110), Natural Science Foundation of Jiangsu (BK20140020 and BK2012310), and Collaborative Innovation Center for Regional Environmental Quality. We would like to thank Shuxiao Wang and Qingru Wu from Tsinghua University for providing detailed technology information of non-ferrous metal smelting, Simon Wilson from Arctic Monitoring and Assessment

ACPD
14, 26803–26855, 2014

The effects of China's pollution control on atmospheric Hg emissions

Y. Zhao et al.

Title Page
Abstract | Introduction
Conclusions | References
Tables | Figures
◀| |▶
◀ ▶
Back | Close
Full Screen / Esc
Printer-friendly Version
Interactive Discussion

Programme for providing the information and data on emissions from artisanal gold production, and Shigeru Suehiro from the International Energy Agency for providing the Chinese energy and industrial projection data.

References

Arctic Monitoring and Assessment Programme (AMAP), and United Nations Environment Programme (UNEP): Technical Background Report for the Global Mercury Assessment, Geneva, Switzerland, 2013.

Chen, C., Wang, H., Zhang, W., Hu, D., Chen, L., and Wang, X.: High-resolution inventory of mercury emissions from biomass burning in China for 2000–2010 and a projection for 2020, J. Geophys. Res., 118, 12248–12256, 2013.

Chen, L., Liu, M., Fan, R., Ma, S., Xu, Z., Ren, M., and He, Q.: Mercury speciation and emission from municipal solid waste incinerators in the Pearl River Delta, South China, Sci. Total Environ., 447, 396–402, 2013.

China Association of Urban Environmental Sanitation (CAUES): Development Report on China Urban Environmental Sanitation (2012), China City Press, Beijing, 2013 (in Chinese).

Ci, Z., Zhang, X., and Wang, Z.: Enhancing atmospheric mercury research in China to improve the current understanding of the global mercury cycle: the need for urgent and closely coordinated efforts, Environ. Sci. Technol., 46, 5636–5642, 2012.

Corbitt, E. S., Jacob, D. J., Holmes, C. D., Streets, D. G., and Sunderland, E. M.: Global source–receptor relationships for mercury deposition under present-day and 2050 emissions scenarios, Environ. Sci. Technol., 45, 10477–10484, 2011.

Cui, X., Ma, L. P., Deng. C. L., Xu. W. J., and Mao. N.: Research progress of removing mercury from coal-fired flue gas, Chemical Industry and Engineering Progress, 30, 1607–1612, 2011(in Chinese).

Feng, X., Sommer, J., Lindqvist, O., and Hong, Y.: Occurrence, emissions and deposition of mercury during coal combustion in the province Guizhou, China, Water Air Soil Poll., 139, 311–324, 2002.

Feng, X., Li, G., and Qiu, G.: A preliminary study on mercury contamination to the environment from artisanal zinc smelting using indigenous methods in Hezhang county, Guizhou, China –

Discussion Paper | Discussion Paper | Discussion Paper | Discussion Paper |

ACPD

14, 26803–26855, 2014

The effects of China's pollution control on atmospheric Hg emissions

Y. Zhao et al.

Part 1: mercury emission from zinc smelting and its influences on the surface waters, Atmos. Environ., 38, 6223–6230, 2004.
Feng, X., Streets, D. G., Hao, J., Wu, Y., and Li, G.: Mercury emissions from industrial sources in China, in: Mercury Fate and Transport in the Global Atmosphere, edited by: Pirrone, N. and Mason, R. P., Springer US, 67–79, 2009.
Frey, H. C. and Zheng, J. Y.: Quantification of variability and uncertainty in air pollutant emission inventories: method and case study for utility NO_X emissions, J. Air Waste Manage., 52, 1083–1095, 2002.
Fu, X., Feng, X., Sommar, J., and Wang, S.: A review of studies on atmospheric mercury in China, Sci. Total Environ., 421–422, 73–81, 2012a.
Fu, X. W., Feng, X., Shang, L. H., Wang, S. F., and Zhang, H.: Two years of measurements of atmospheric total gaseous mercury (TGM) at a remote site in Mt. Changbai area, Northeastern China, Atmos. Chem. Phys., 12, 4215–4226, doi:10.5194/acp-12-4215-2012, 2012a.
Guo, Y., Yan, N., Yang, S., Qu, Z., Wu, Z., Liu, Y., Liu, P., and Jia, J.: Conversion of elemental mercury with a novel membrane delivery catalytic oxidation system, Environ. Sci. Technol., 45, 706–711, 2011.
Hao, C., Shen, Y., and Zhang, Y.: Study on mercury consumption reduction plans for PVC resin industry in China, Research of Environmental Sciences, 18, 112–115, 2005 (in Chinese).
Hong, B., Zhu, Y., Feng, X., and Wang, Y.: Distribution of mercury in coal gas generating procedure, Earth Env. Sci. T. R. So., 32, 12–16, 2004 (in Chinese).
Hu, D., Zhang, W., Chen, L., Chen, C., Ou, L., Tong, Y., Wei, W., Long, W., and Wang, X.: Mercury emissions from waste combustion in China from 2004 to 2010, Atmos. Environ., 62, 359–366, 2012.
Huang, W. and Yang, Y.: Mercury in coal in China, Coal Geology of China, 14, 37–40, 2002 (in Chinese).
Huang, X., Li, M., Friedli, H. R., Song, Y., Chang, D., and Zhu, L.: Mercury emissions from biomass burning in China, Environ. Sci. Technol., 45, 9442–9448, 2011.
Huang, Y., Jin, B., Zhong, Z., and Xiao, R.: Study on the distribution of trace elements in gasification products, Proceedings of the CSEE, 24, 208–212, 2004 (in Chinese).
International Energy Agency (IEA): World Energy Outlook 2012, International Energy Agency, Paris, France, 2012
Ito, S., Yokoyama, T., and Asakura, K.: Emissions of mercury and other trace elements from coal-fired power plants in Japan, Sci. Total Environ., 368, 397–402, 2006.

ACPD
14, 26803–26855, 2014

Lei, Y., Zhang, Q., Nielsen, C. P., and He, K. B.: An inventory of primary air pollutants and CO_2 emissions from cement industry in China, 1990–2020, Atmos. Environ., 45, 147–154, 2011.
Li, G., Feng, X., and Li, Z.: Atmospheric mercury emissions from retort Zn productions, J. Tsinghua Univ. (Sci & Tech), 49, 2001–2004, 2009 (in Chinese).
Li, G., Feng, X., Li, Z., Qiu, G., Shang, L., Liang, P., Wang, D., and Yang, Y.: Mercury emission to atmosphere from primary Zn production in China, Sci. Total Environ., 408, 4607–4612, 2010.
Li, P., Feng, X., Qiu, G., Shang, L., Wang, S., and Meng, B.: Atmospheric mercury emission from artisanal mercury mining in Guizhou Province, Southwestern China, Atmos. Environ., 43, 2247–2251, 2009.
Li, P., Feng, X., Qiu, G., Shang, L., and Wang, S.: Mercury pollution in Wuchuan mercury mining area, Guizhou, Southwestern China: the impacts from large scale and artisanal mercury mining, Environ. Int., 42, 59–66, 2012.
Li, W.: Characterization of Atmospheric Mercury Emissions from Coal-fired Power Plant and Cement Plant (Master Thesis), Xi'nan University, Chongqing, China, 2011 (in Chinese).
National Bureau of Statistics (NBS): China Statistical Yearbook 2005–2012, China Statistics Press, Beijing, 2013a (in Chinese).
National Bureau of Statistics (NBS): China Industry Economy Statistical Yearbook 2005–2012, China Statistics Press, Beijing, 2013b (in Chinese).
National Bureau of Statistics (NBS): China Statistical Yearbook 2005–2012, China Statistics Press, Beijing, 2013c (in Chinese).
Pacyna, E. G. and Pacyna, J. M.: Global emission of mercury from anthropogenic sources in 1995, Water Air Soil Poll., 137, 149–165, 2002.
Pacyna, E. G., Pacyna, J. M., Sundseth, K., Munthe, J., Kindbom, K., Wilson, S., Steenhuisen, F., and Maxson, P.: Global emission of mercury to the atmosphere from anthropogenic sources in 2005 and projections to 2020, Atmos. Environ., 44, 2487–2499, 2010.
Pirrone, N. and Mason, R. P.: Mercury Fate and Transport in the Global Atmosphere, Springer US, 2009.
Pirrone, N., Cinnirella, S., Feng, X., Finkelman, R. B., Friedli, H. R., Leaner, J., Mason, R., Mukherjee, A. B., Stracher, G. B., Streets, D. G., and Telmer, K.: Global mercury emissions to the atmosphere from anthropogenic and natural sources, Atmos. Chem. Phys., 10, 5951–5964, doi:10.5194/acp-10-5951-2010, 2010.

ACPD
14, 26803–26855, 2014

Slemr, F., Brunke, E.-G., Ebinghaus, R., and Kuss, J.: Worldwide trend of atmospheric mercury since 1995, Atmos. Chem. Phys., 11, 4779–4787, doi:10.5194/acp-11-4779-2011, 2011.
Srivastava, R. K., Hutson, N., Martin, B., Princiotta, F., and Staudt, J.: Control of mercury emissions from coal-fired electric utility boilers, Environ. Sci. Technol., 40, 1385–1393, 2006.
Streets, D. G., Hao, J., Wu, Y., Jiang, J., Chan, M., Tian, H., and Feng, X.: Anthropogenic mercury emissions in China, Atmos. Environ., 39, 7789–7806, 2005.
Streets, D. G., Zhang, Q., and Wu, Y.: Projections of global mercury emissions in 2050, Environ. Sci. Technol., 43, 2983–2988, 2009a.
Streets, D. G., Hao. J., Wang, S., and Wu, Y.: Mercury emissions from coal combustion in China, in: Mercury Fate and Transport in the Global Atmosphere, edited by: Pirrone, N. and Mason, R. P., Springer US, 51–65, 2009b.
Tang, S., Feng, X., Shang, L., Yan, H., and Hou, Y.: Mercury speciation and emissions in the flue gas of a small-scale coal-fired boiler in Guiyang, Research of Environmental Sciences, 17, 74–76, 2004 (in Chinese).
Tian, H. Z., Wang, Y., Xue, Z. G., Cheng, K., Qu, Y. P., Chai, F. H., and Hao, J. M.: Trend and characteristics of atmospheric emissions of Hg, As, and Se from coal combustion in China, 1980–2007, Atmos. Chem. Phys., 10, 11905–11919, doi:10.5194/acp-10-11905-2010, 2010.
Tian, H., Wang, Y., Cheng, K., Qu, Y., Hao, J, Xue, Z., and Chai, F.: Control strategies of atmospheric mercury emissions from coal-fired power plants in China, J. Air Waste Manage., 62, 576–58, 2012.
Tsinghua University (THU): Improve the Estimates of Anthropogenic Mercury Emissions in China, Technical report, available at: http://ww.chem.unep.ch/MERCURY/, 2009.
United Nations Economic Commission for Europe/The European Monitoring and Evaluation Programme (UNECE/EMEP): Atmospheric Emission Inventory Guidebook, available at: http://reports.eea.eu.int/EMEPCORINAIR4/en/page002.html, 2004.
U.S. Environmental Protection Agency (USEPA): Compilation of Air Pollutant Emission Factors (AP-42), available at: http://www.epa.gov/ttn/chief/ap42/index.html, 2002a.
U.S. Environmental Protection Agency (USEPA): Characterization and Management of Residues From Coal-Fired Power Plants, Interim Report, EPA-600/R-02-083, 2002b.
U.S. Geological Survey (USGS): Mercury Content in Coal Mines in China (unpublished data), 2004.

ACPD
14, 26803–26855, 2014

Wan, Q., Feng, X., Lu, J., Zheng, W., Song, X., Han, S., and Xu, H.: Atmospheric mercury in Changbai Mountain area, northeastern China – Part 1: the seasonal distribution pattern of total gaseous mercury and its potential sources, Environ. Res., 109, 201–206, 2009.

Wang, F.: The control policy for total emission amount of primary pollutants during the 12th Five Year Plan period, presented at the 17th Workshop on SO_2, NO_X, and Hg pollution control technology and $PM_{2.5}$ control and monitoring technology, Hangzhou, China, 16–17 May 2013.

Wang, K., Wang, C., Lu, X. D., and Chen, J. N.: Scenario analysis on CO_2 emissions reduction potential in China's iron and steel industry, Energ. Policy, 35, 2320–2335, 2007.

Wang, L., Wang, S., Zhang, L., Wang, Y., Zhang, Y., Nielsen, C., McElroy, M. B., and Hao, J.: Source apportionment of atmospheric mercury pollution in China using the GEOS-Chem model, Environ. Pollut., 190, 166–175, 2014.

Wang, Q., Shen, W., and Ma, Z.: Estimation of mercury emission from coal combustion in China, Environ. Sci. Technol., 34, 2711–2713, 2000.

Wang, S. X., Song, J. X., Li, G. H., Wu, Y., Zhang, L., Wan, Q., Streets, D. G., Chin, C. K., and Hao, J. M.: Estimating mercury emissions from a zinc smelter in relation to China's mercury control policies, Environ. Pollut., 158, 3347–3353, 2010a.

Wang, S. X., Zhang, L., Li, G. H., Wu, Y., Hao, J. M., Pirrone, N., Sprovieri, F., and Ancora, M. P.: Mercury emission and speciation of coal-fired power plants in China, Atmos. Chem. Phys., 10, 1183–1192, doi:10.5194/acp-10-1183-2010, 2010b.

Wang, S. X., Zhang, L., Wu, Y., Ancora, M. P., Zhao, Y., and Hao, J. M.: Synergistic mercury removal by conventional pollutant control strategies for coal-fired power plants in China, J. Air Waste Manage., 60, 722–730, 2010c.

Wang, S. X., Zhang, L., Zhao, B., Meng, Y., and Hao, J. M.: Mitigation potential of mercury emissions from coal-fired power plants in China, Energy Fuels, 26, 4635–4642, 2012.

Wang, W. X.: Analysis of energy consumption and energy saving potential for iron and steel industry, China Steel, 4, 19–22, 2011 (in Chinese).

Wu, Q. R., Wang, S. X., Zhang, L., Song, J. X., Yang, H., and Meng, Y.: Update of mercury emissions from China's primary zinc, lead and copper smelters, 2000–2010, Atmos. Chem. Phys., 12, 11153–11163, doi:10.5194/acp-12-11153-2012, 2012.

Wu, Y., Wang, S., Streets, D. G., Hao, J., Chan, M., and Jiang. J.: Trends in anthropogenic mercury emissions in China from 1995 to 2003, Environ. Sci. Technol., 40, 5312–5318, 2006.

ACPD
14, 26803–26855, 2014

The effects of China's pollution control on atmospheric Hg emissions

Y. Zhao et al.

Wu, Y., Streets, D. G., Wang, S. X., and Hao, J. M.: Uncertainties in estimating mercury emissions from coal-fired power plants in China, Atmos. Chem. Phys., 10, 2937–2946, doi:10.5194/acp-10-2937-2010, 2010.

Xu, Y.: Improvements in the operation of SO_2 scrubbers in China's coal power plants, Environ. Sci. Technol., 45, 380–385, 2011.

Yao, W., Qu, X., Li, H., and Fu, Y.: Production, collection and treatment of garbage in rural areas in China, J. Environ. Health, 26, 10–12, 2009 (in Chinese).

Yan, N., Chen, W., Chen, J., Qu, Z., Guo, Y., Yan, S., and Jia, J.: Significance of RuO2 modified SCR catalyst for elemental mercury oxidation in coal-fired flue gas, Environ. Sci. Technol., 45, 5725–5730, 2011.

Zhang, L.: Research on Mercury Emission Measurement and Estimate From Combustion Resources (Master Thesis), Zhejiang University, Hangzhou, China, 2007 (in Chinese).

Zhang, L., Zhuo, Y., Chen, L., Xu, X., and Chen, C.: Mercury emissions from six coal-fired power plants in China, Fuel Process. Technol., 89, 1033–1040, 2008.

Zhang, L., Wang, S., Meng, Y., and Hao, J.: Influence of mercury and chlorine content of coal on mercury emissions from coal-fired power plants in China, Environ. Sci. Technol., 46, 6385–6392, 2012a.

Zhang, L., Wang, S., Wu, Q., Meng, Y., Yang, H., Wang, F., and Hao, J.: Were mercury emission factors for Chinese non-ferrous metal smelters overestimated? Evidence from onsite measurements in six smelters, Environ. Pollut., 171, 109–117, 2012b.

Zhang, W., Wei, W., Hu, D., Zhu, Y., and Wang, X.: Emission of speciated mercury from residential biomass fuel combustion in China, Energy Fuels, 27, 6792–6800, 2013.

Zhao, Y., Wang, S. X., Duan, L., Lei, Y., Cao, P. F., and Hao, J. M.: Primary air pollutant emissions of coal-fired power plants in China: current status and future prediction, Atmos. Environ., 42, 8442–8452, 2008.

Zhao, Y., Wang, S. X., Nielsen, C. P., Li, X. H., and and Hao, J. M.: Establishment of a database of emission factors for atmospheric pollutants from Chinese coal-fired power plants, Atmos. Environ., 44, 1515–1523, 2010.

Zhao, Y., Nielsen, C. P., Lei, Y., McElroy, M. B., and Hao, J.: Quantifying the uncertainties of a bottom-up emission inventory of anthropogenic atmospheric pollutants in China, Atmos. Chem. Phys., 11, 2295–2308, doi:10.5194/acp-11-2295-2011, 2011.

Zhao, Y., Nielsen, C. P., McElroy, M. B., Zhang, L., and Zhang, J.: CO emissions in and China: uncertainties and implications of improved energy efficiency and emission control, Atmos. Environ., 49, 103–113, 2012.
Zhao, Y., Zhang, J., and Nielsen, C. P.: The effects of recent control policies on trends in emissions of anthropogenic atmospheric pollutants and CO_2 in China, Atmos. Chem. Phys., 13, 487–508, doi:10.5194/acp-13-487-2013, 2013.
Zhao, Y., Zhang, J., and Nielsen, C. P.: The effects of energy paths and emission controls and standards on future trends in China's emissions of primary air pollutants, Atmos. Chem. Phys., 14, 8849–8868, doi:10.5194/acp-14-8849-2014, 2014.
Zhi, G., Xue, Z., Li, Y., Ma, J., Liu, Y., Meng, F., and Chai, F.: Uncertainty of flue gas mercury emissions from coal-fired power plants in China based on field measurements, Research of Environmental Sciences, 26, 814–821, 2013 (in Chinese).

ACPD
14, 26803–26855, 2014

Table 1. Uncertainties of Hg emission factors for main sources, expressed as the probability distribution functions (PDF).

Parameters		Samples	Distribution	Key characteristics for distribution functions		
				P10[a]/Min[b]	P90[a]/Max[b]	Mean[a]/Most likely[b]
Release rates of boilers for CPP, %						
PC		32	Triangular	89	100	99
Grate		2	Triangular	92	100	96
CFB		3	Triangular	93	100	98
Release rates of boilers for OIB/HB/FOS, %						
Grate		3	Triangular	51	91	76
CFB		1	Triangular	51	100	91
Hg removal efficiency by APCDs for CPP, %						
FF		5	Weibull	21	84	56
ESP		44	Normal	18	23	20
WET		3	Weibull	4	26	13
FGD+ESP		30	Weibull	40	68	57
CYC		3	Uniform	0	14	–
SCR		7	Triangular	10	100	77
CFB+ESP		3	Weibull	18	60	43
Nonferrous metal smelting [c]						
Zinc	EP	6	Triangular	0	45	9
	ISP	3	Uniform	0	140	–
	RZSP	2	Uniform	2	38	–
	AZSP	4	Triangular	4	203	89
Lead	RPSP	2	Uniform	0	1.4	–
	SMP	2	Uniform	0	12	–
Copper	FFSP	2	Uniform	0	0.3	–
	RPSP	2	Uniform	0.1	0.3	–
Cement production						
FF		7	Weibull	0.006	0.011	0.008
ESP		2	Uniform	0.01	0.11	–
WET/CYC		2	Uniform	0.06	0.18	–
Biofuel use/biomass open burning						
Firewood		26	Uniform	0	50	–
Crops		9	Uniform	0	106	–
Waste incineration						
Municipal		29	Weibull	0.21	0.32	0.27
Rural	Release rates	1	Normal	0.37	0.63	0.5
	Hg content	31	Weibull	0.12	1.58	0.6

[a] P10 values mean that there is a probability of 10 % that the actual result would be equal to or below the P10 values; P50 mean that there is a probability of 50 % that the actual result would be equal to or below the P50 values; and P90 mean that there is a probability of 90 % that the actual result would be equal to or below the P90 values.
[b] These values are for the minimum, the most likely, and the maximum values for the triangular distribution function instead of P10, P50, and P90 values, or for the minimum and maximum values for the uniform distribution function instead of P10 and P90 values.
[c] Full names of manufacturing technologies: EP: electrolytic process; ISP: imperial smelting process; RZSP: retort zinc smelting process; AZ: artisanal zinc smelting process; RPSP: rich-oxygen pool smelting process; SMP: sinter machine process; and FFSP: flash furnace smelting process.

Table 2. Uncertainties of mass fractions of Hg speciation for main sources.

Parameters		Samples	Distribution	Key characteristics for distribution functions/%		
				P10/Min	P90/Max	Mean/Most likely
FF	Hg^0	4	Triangular	4.8	30.6	15.8
	Hg^p	4	Triangular	0.0	34.8	10.8
ESP	Hg^{2+}	20	Normal	27.9	42.4	35.2
	Hg^p	20	Triangular	0.0	3.6	0.22
FGD+ESP	Hg^{2+}	11	Normal	9.8	22.2	16.0
	Hg^p	11	Triangular	0.0	3.7	0.3
WET	Hg^0	2	Uniform [b]	0.0	60.0	–
	Hg^p	2	Uniform [b]	0.0	28.0	–
NOC [a]	Hg^0	–	Uniform [b]	0.0	48.0	–
	Hg^{2+}	–	Uniform [b]	0.0	40.0	–
SCR	Hg^{2+}	6	Triangular	15.7	40.6	27.6
NMS_Zn	Hg^0	3	Triangular	0.0	55.0	29.0
	Hg^p	3	Uniform	0.0	5.0	–
NMS_Pb	Hg^{2+}	2	Triangular	15.0	65.0	40.0
NMS_Cu	Hg^{2+}	2	Uniform	28.0	72.0	–
BIO	Hg^0	25	Weibull	57.3	94.2	76.9
	Hg^{2+}	25	Triangular	0.0	21.7	5.0
SWI	Hg^0	10	Gamma	1.1	33.8	6.2
	Hg^p	10	Gamma	0.1	2.6	0.5

[a] No control device for coal combustion.
[b] Tentatively assumed.

ACPD
14, 26803–26855, 2014

The effects of China's pollution control on atmospheric Hg emissions

Y. Zhao et al.

Table 3. National Hg emissions by source category from 2005 to 2012.

Source category	2005	2006	2007	2008	2009	2010	2011	2012
Coal-fired power plants	**144.7**	**149.5**	**152.5**	**144.2**	**140.6**	**140.0**	**155.8**	**143.6**
Industry	**473.0**	**495.9**	**530.0**	**533.8**	**546.0**	**542.3**	**540.3**	**526.4**
Cement production	64.4	65.8	66.8	59.1	59.4	45.7	40.1	40.0
Coal use	16.1	17.6	18.7	18.0	20.0	20.4	21.5	22.2
Iron and steel plants	26.2	28.0	28.2	29.7	32.3	34.8	36.8	37.6
Heating boilers	18.1	20.5	24.1	26.0	26.3	30.1	32.6	34.5
Other industrial boilers	61.2	66.7	76.0	81.6	83.7	80.6	87.9	87.4
Nonferrous metal smelting	87.4	98.1	114.2	108.1	112.7	117.6	105.1	91.4
Zinc	43.0	49.0	58.3	59.2	63.4	72.2	69.9	68.1
Lead	39.9	45.0	52.4	45.6	45.8	41.9	34.0	22.0
Copper	4.5	4.1	3.4	3.4	3.5	3.5	1.2	1.4
Gold metallurgy	184.4	183.8	183.8	182.3	183.3	179.5	181.0	182.6
Large scale	17.7	17.1	17.1	15.6	16.6	12.8	14.3	15.9
Artisanal and small scale	166.7	166.7	166.7	166.7	166.7	166.7	166.7	166.7
Other miscellaneous processes	31.2	33.1	37.0	47.0	48.4	54.1	56.8	52.9
Mercury mining	16.2	13.5	14.2	23.7	25.3	28.2	28.3	24.0
Battery/fluorescent lamp production	7.6	8.7	9.8	10.9	10.0	10.0	10.0	10.0
PVC production	7.0	8.8	10.7	10.0	10.7	13.6	16.0	16.3
Oil and gas combustion	0.5	2.1	2.3	2.3	2.4	2.4	2.6	2.6
Residential and commercial sector	**61.3**	**59.8**	**61.4**	**63.6**	**67.8**	**70.7**	**74.2**	**79.5**
Coal burning	30.0	28.0	27.2	30.7	33.0	34.9	36.5	38.5
Biofuel use/biomass open burning	10.3	10.5	9.7	9.2	9.4	8.2	8.3	8.4
Solid waste incineration	10.3	10.9	11.4	11.6	12.4	12.8	13.3	15.3
Municipal	1.7	2.5	3.2	3.5	4.4	5.1	5.7	7.9
Rural	8.6	8.4	8.2	8.1	7.9	7.7	7.6	7.4
Oil and gas combustion	10.7	10.4	13.1	12.1	13.0	14.9	16.1	17.4
Total	**679.0**	**705.2**	**743.8**	**741.7**	**754.4**	**753.0**	**770.3**	**749.5**
Total coal combustion	**296.2**	**310.2**	**326.6**	**330.3**	**335.9**	**340.7**	**371.1**	**363.8**

ACPD
14, 26803–26855, 2014
The effects of China's pollution control on atmospheric Hg emissions
Y. Zhao et al.

Table 4. Uncertainties of Hg emissions by sector for 2005, 2008, 2010 and 2012, expressed as the 95 % confidence intervals of central estimates. The unit for emissions is metric tons (t).

	2005	2008	2010	2012
CPP	145 (−48 %, +73 %)	144 (−50 %, +70 %)	140 (−51 %, +77 %)	144 (−50 %, +89 %)
IND	473 (−30 %, +43 %)	534 (−27 %, +46 %)	543 (−26 %, +51 %)	527 (−27 %, +54 %)
RES	61 (−36 %, +144 %)	64 (−35 %, +127 %)	71 (−34 %, +123 %)	79 (−35 %, +115 %)
Total	679 (−26 %, +46 %)	742 (−24 %, +46 %)	753 (−23 %, +51 %)	750 (−23 %, +53 %)
Total [a]	512 (−25 %, +55 %)	575 (−24 %, +56 %)	586 (−23 %, +61 %)	583 (−24 %, +65 %)
Coal	296 (−48 %, +70 %)	330 (−49 %, +66 %)	341 (−49 %, +69 %)	364 (−48 %, +76 %)

[a] Emissions from ASGM excluded.

ACPD
14, 26803–26855, 2014

Table 5. The parameters contributing most to emission uncertainties by sector for 2010. The percentages in the parentheses indicate the contributions of the parameters to the variance of corresponding emission estimates.

	CPP	IND	RES
Hg	$\eta_{ESP+FGD}$ (26 %) $HgC_{Shandong}$ (21 %)	E_{ASGM} (41 %) $EF_{NMS\_Zn, EP}$ (17 %)	EF_{straw} (26 %) AL_{coal} (14 %)
Hg^0	$HgC_{Shandong}$ (18 %) HgC_{Henan} (8 %)	E_{ASGM} (39 %) $f_{GM, Hg2+}$ (19 %)	EF_{straw} (41 %) AL_{straw} (12 %)
Hg^{2+}	$HgC_{Shandong}$ (20 %) $f_{ESP+FGD, Hg2+}$ (13 %)	$f_{GM, Hg2+}$ (28 %) $EF_{NMS\_Zn, EP}$ (22 %)	HgC_{waste} (28 %) $f_{NOC, Hg2+}$ (8 %)
Hg^p	$f_{ESP+FGD, Hgp}$ (30 %) $f_{FF, Hgp}$ (14 %)	$f_{WET, Hgp}$ (74 %) $HgC_{Shandong}$ (4 %)	AL_{coal} (22 %) $f_{NOC, Hg0}$ (15 %)

ACPD
14, 26803–26855, 2014

Table 6. Projection of national Hg missions by source category for different scenarios through 2030.

Source category	2015			2020			2030		
	S0	S1	S2	S0	S1	S2	S0	S1	S2
Coal-fired power plants	**150.0**	**149.6**	**130.8**	**164.2**	**153.1**	**130.9**	**181.8**	**155.0**	**126.8**
Industry	**578.1**	**571.1**	**405.4**	**588.0**	**580.9**	**401.4**	**570.9**	**547.6**	**342.5**
Cement production	36.8	36.6	25.4	37.5	37.3	17.2	25.0	24.3	8.9
Coal use	21.1	21.0	13.2	21.7	21.6	11.3	17.6	17.3	8.7
Iron and steel plants	40.0	39.9	39.3	41.7	41.4	39.0	39.8	39.1	34.8
Heating boilers	39.2	37.8	34.2	38.8	37.4	33.8	40.8	36.1	32.3
Other industrial boilers	105.2	101.3	86.4	104.1	100.4	85.4	109.4	96.8	81.7
Nonferrous metal smelting	110.5	109.6	102.4	116.0	115.0	105.5	109.6	106.8	68.2
Zinc	84.5	83.8	78.9	88.7	88.0	81.8	83.8	81.7	56.0
Lead	24.7	24.5	22.3	25.9	25.7	22.4	24.5	23.9	11.0
Copper	1.3	1.3	1.2	1.4	1.3	1.3	1.3	1.3	1.2
Gold metallurgy	182.5	182.4	63.3	183.3	183.1	63.7	182.4	182.0	63.2
Large scale	15.5	15.4	7.7	16.3	16.1	8.1	15.4	15.0	7.5
Artisanal and small scale	167.0	167.0	55.7	167.0	167.0	55.7	167.0	167.0	55.7
Other miscellaneous processes	64.0	63.5	54.3	66.6	66.1	56.7	63.9	62.6	53.4
Mercury mining	34.1	33.8	33.8	35.8	35.5	35.5	33.8	33.0	33.0
Battery/fluorescent lamp production	10.0	10.0	3.3	10.0	10.0	3.3	10.0	10.0	3.3
PVC production	16.8	16.7	14.1	17.7	17.5	14.8	16.7	16.3	13.7
Oil and gas combustion	3.0	3.0	3.0	3.2	3.1	3.1	3.3	3.3	3.3
Residential and commercial sector	**86.0**	**84.2**	**84.2**	**92.0**	**88.4**	**88.4**	**116.7**	**109.9**	**109.9**
Coal burning	37.9	37.0	37.0	37.3	36.4	36.4	34.6	31.6	31.5
Biofuel use/biomass open burning	8.7	8.7	8.7	8.1	8.1	8.1	6.6	6.6	6.6
Solid waste incineration	20.7	20.7	20.7	24.6	24.6	24.6	49.7	49.7	49.7
Municipal	13.9	13.9	13.9	18.5	18.5	18.5	45.1	45.1	45.1
Rural	6.8	6.8	6.8	6.1	6.1	6.1	4.6	4.6	4.6
Oil and gas combustion	18.7	17.8	17.8	22.0	19.3	19.3	25.8	22.0	22.0
Total	**814.1**	**805.0**	**620.4**	**844.3**	**822.5**	**620.7**	**869.3**	**812.5**	**579.1**
Total coal combustion	**393.3**	**386.7**	**340.9**	**407.9**	**390.4**	**336.9**	**423.9**	**375.9**	**315.8**

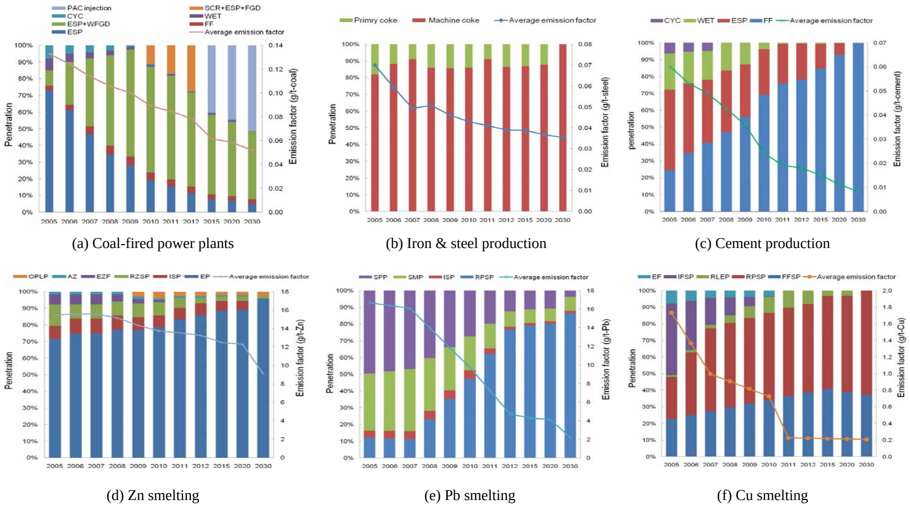

Figure 1. The penetrations of technologies and inter-annual trends of Hg emission factors for typical sources in China for 2005–2012 and S2 till 2030. In each panel, left-hand vertical axis indicates the percentages of various technologies and right-hand vertical axis indicates the emission factors.

ACPD
14, 26803–26855, 2014

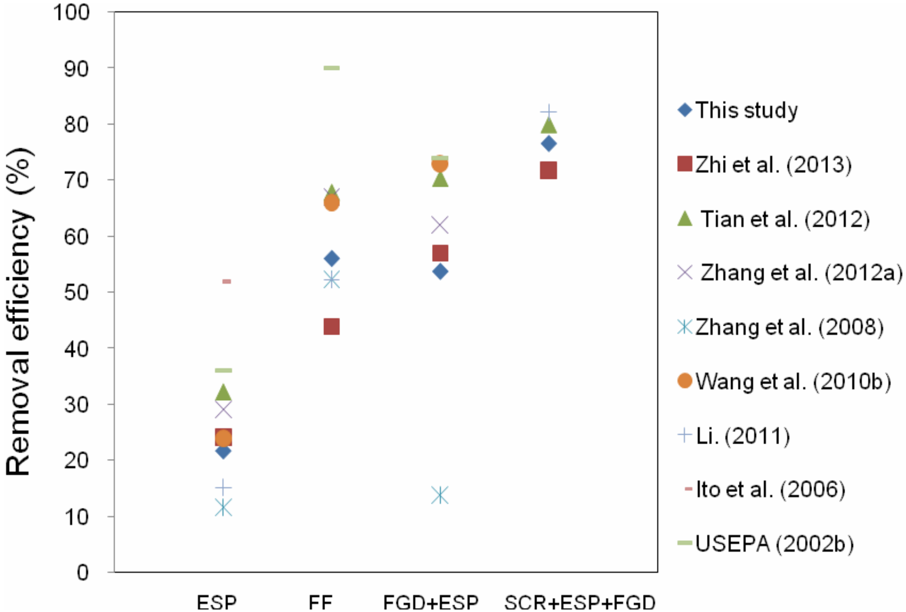

Figure 2. Mercury removal efficiencies of different APCD combinations estimated in this work, compared with other inventory studies.

ACPD
14, 26803–26855, 2014

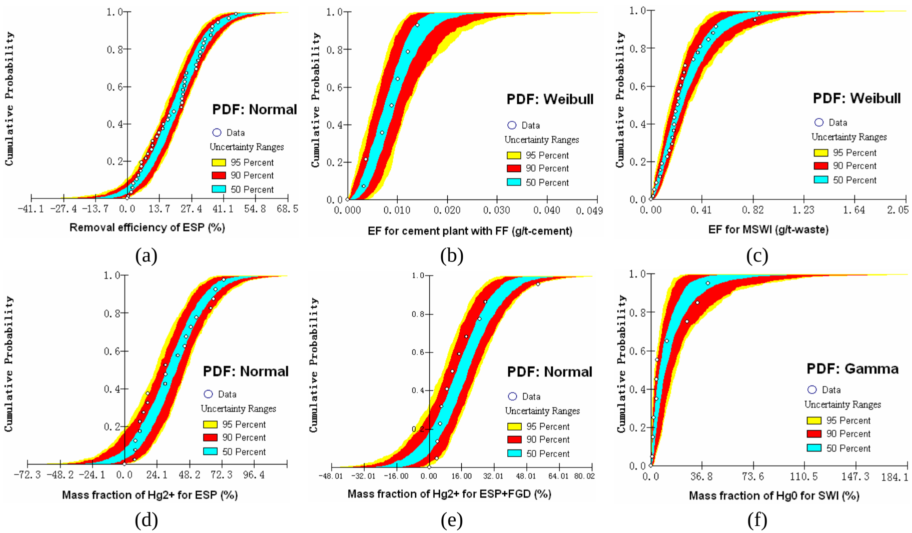

Figure 3. Bootstrap analysis for given parameters of Hg emission factor estimate, expressed as the probability bands with PDF indicated in each panel.

ACPD

14, 26803–26855, 2014

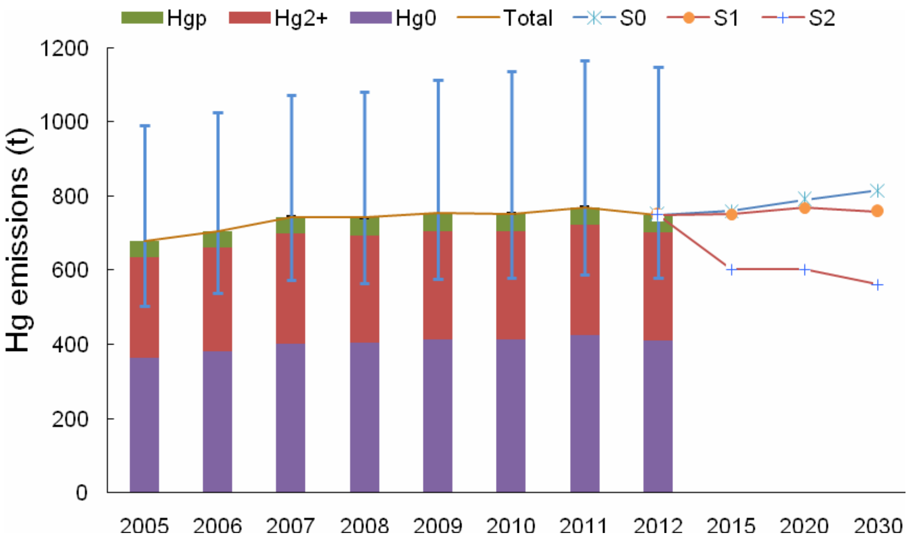

Figure 4. National total Hg emissions with speciation from 2005 to 2012 and future trends under three scenarios through 2030. The error bars for 2005–2012 indicate the 95 % confidence intervals of the annual total emission estimates.

ACPD
14, 26803–26855, 2014

The effects of China's pollution control on atmospheric Hg emissions

Y. Zhao et al.

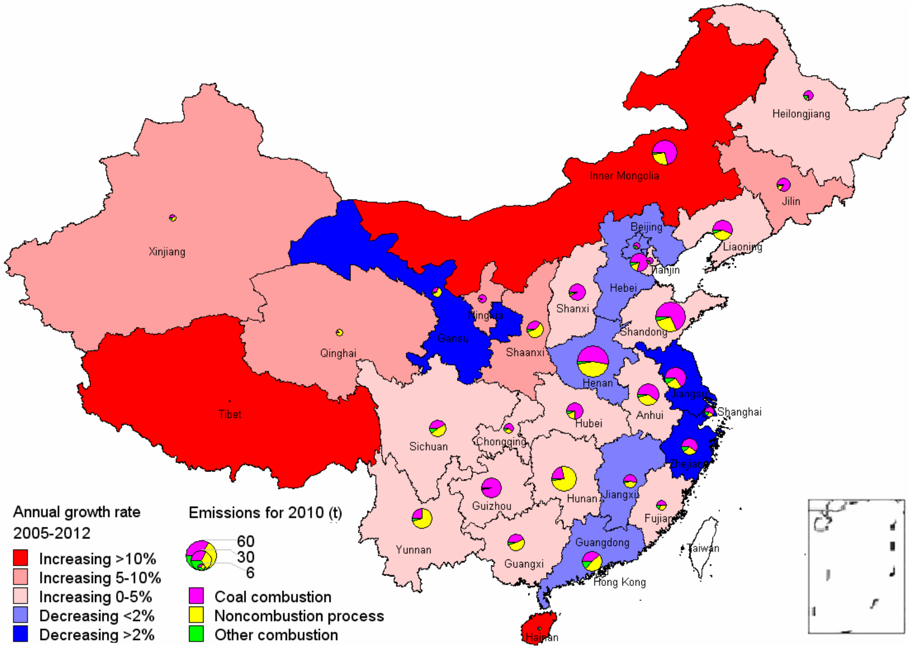

Figure 5. Provincial Hg emissions in 2010 and the relative changes between 2005 and 2012. The sizes of the pie graphs indicate absolute emissions by source in 2010. Emissions from ASGM are excluded.

ACPD
14, 26803–26855, 2014

The effects of China's pollution control on atmospheric Hg emissions

Y. Zhao et al.

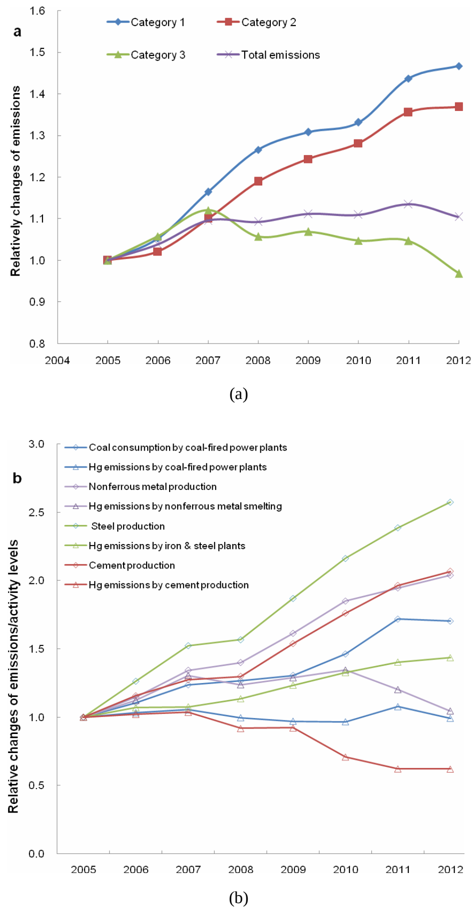

Figure 6. (a) Relatively changes in Hg emissions of national total and different source categories, and **(b)** relatively changes of Hg emissions and activity levels for given sectors (all the values are normalized to the levels in 2005).

ACPD
14, 26803–26855, 2014

The effects of China's pollution control on atmospheric Hg emissions

Y. Zhao et al.

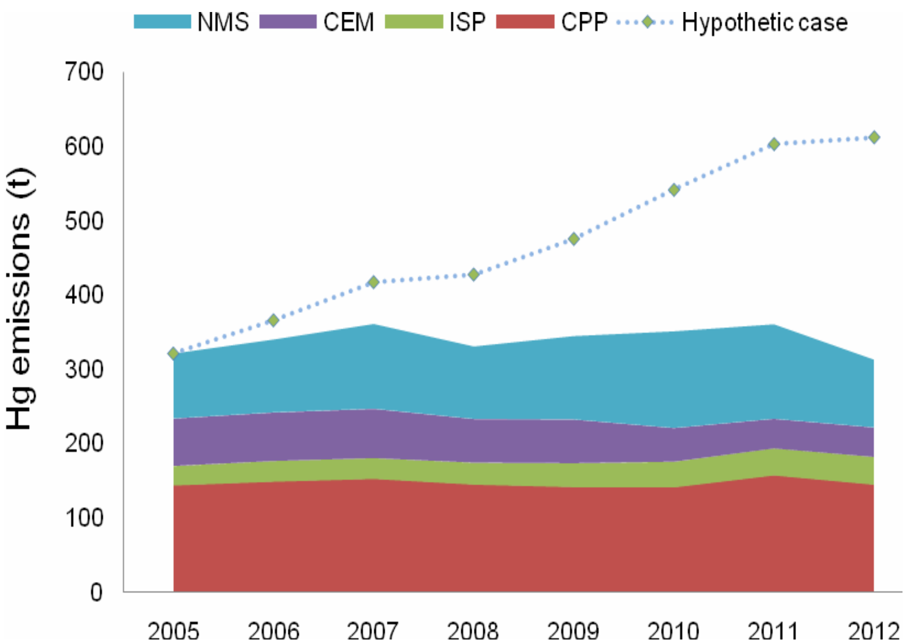

Figure 7. Benefits of pollution control on Hg emission abatement for given sectors from 2005 to 2012.

ACPD
14, 26803–26855, 2014

The effects of China's pollution control on atmospheric Hg emissions

Y. Zhao et al.

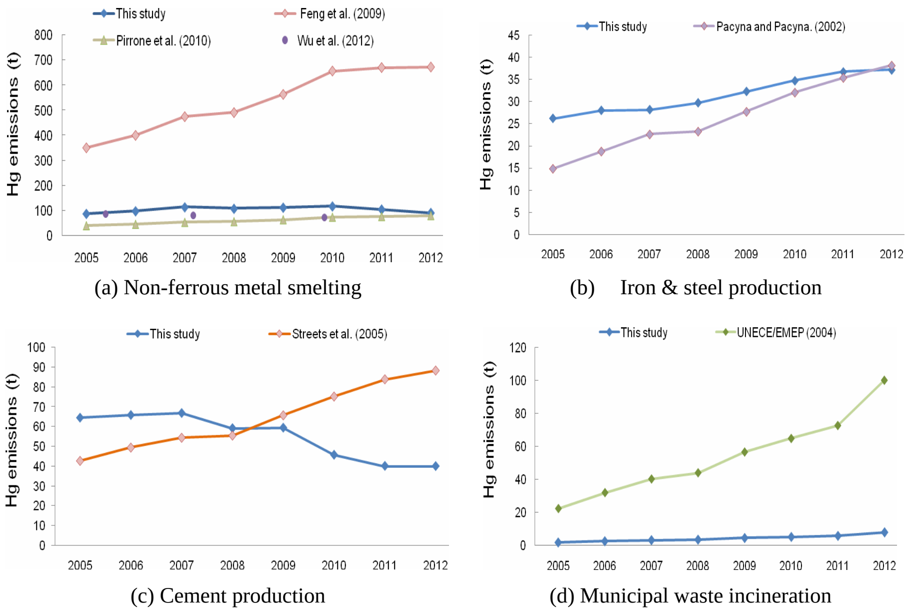

Figure 8. Comparison of Hg emission estimates w/o updated dynamic emission factors for **(a)** nonferrous metal smelting, **(b)** iron and steel production, **(c)** cement production, and **(d)** solid waste incineration. Note all the estimates of cited studies except for Wu et al. (2012) are not directly obtained from the literatures, but are recalculated based on the same emission factors suggested by those studies.

ACPD
14, 26803–26855, 2014

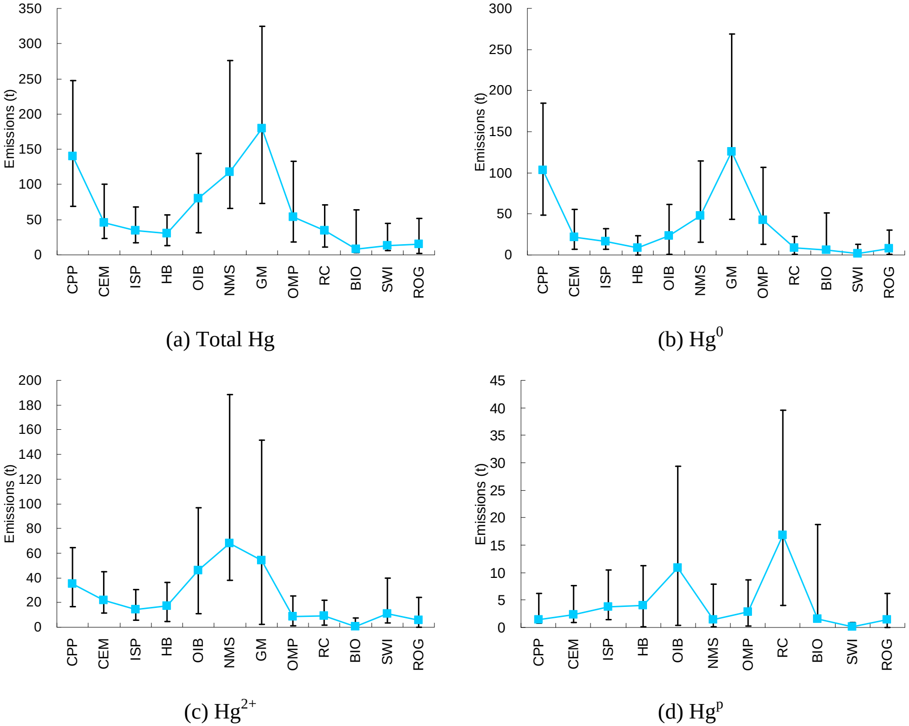

Figure 9. Uncertainties of China's Hg emission estimate by source for 2010: **(a)** total Hg; **(b)** Hg^0; **(c)** Hg^{2+}; and **(d)** Hg^p.

ACPD
14, 26803–26855, 2014

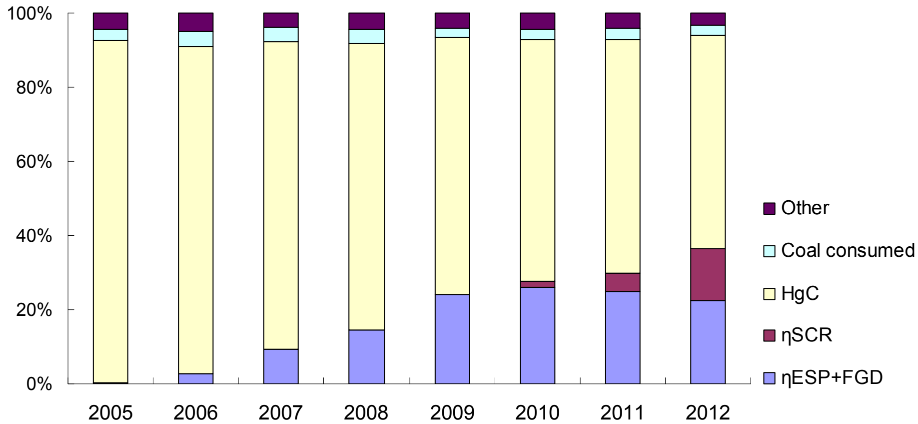

Figure 10. Contribution of different parameters to variance of Hg emissions from CPP during 2005–2012.